SYNTHESIS AND CHARACTERIZATION OF LACTIC ACID-MAGNESIUM OXIDE NANOCOMPOSITES: HOW NANOPARTICLE SIZE AND SHAPE EFFECTS POLYMERIZATION AND THE RESULTING PROPERTIES OF THE POLYMER

by

ERIN M. BEAVERS

B.S., Emporia State University, 2005

A THESIS

submitted in partial fulfillment of the requirements for the degree

MASTER OF SCIENCE

Department of Chemistry
College of Arts and Science

KANSAS STATE UNIVERSITY
Manhattan, Kansas

2008

Approved by:

Major Professor
Kenneth J. Klabunde

Copyright

Abstract

In this study, low molecular weight nanocomposites of l-lactic acid were synthesized with Commercial, Nanoactive®, and Nanoactive Magnesium Oxide Plus®, each of which differs in both surface area and shape. Synthesis of the composites was carried out by refluxing the nanoparticles in a solvent suspension. Both methanol and 1-propanol were used during this work. Reflux was necessary in order to achieve adequate dispersion of the particles before adding l-lactic acid. Upon addition of the lactic acid monomer, the reactants were refluxed for a total of 3 hours, followed by evaporation of the excess solvent.

The products were characterized via DSC, TGA, FTIR, ^{1}H and ^{13}C NMR, UV-Vis, XRD, and TEM. Additionally, titrations were performed with the reactants to ensure the particles were not being consumed by the acid regardless of their size. The results of this study indicate that condensation reactions are the primary polymerization route of lactic acid and polymerization appears to initiate on the surface of the magnesium oxide particles, the result of which are physically unique composites of lactic acid and magnesium oxide.

Table of Contents

List of Figures

List of Tables

Acknowledgements

To my family, Matthew, Noah, Mom & Dad, Mick, Gary & Connie, John & Amanda – thank you for all of the support, encouragement, and understanding you have provided me during my time at Kansas State.

To my advisor, Dr. Kenneth Klabunde – thank you for the patience and understanding you have shown while I have been here. I will forever be grateful to have worked under the guidance of the "Toxic Avenger".

To Dr. Jim Roach – thank you for suggesting graduate school and for convincing me to go, and of course for all of those fabulous P-chem lab reports!

To my committee members, Dr. Susan Sun, Dr. Duy Hua, and Dr. Chris Levy – thank you for all the time, suggestions, and guidance you have given me throughout the course of this work.

To my labmates, Dr. Dima Demydov, Dr. Johanna Haggstrom, Aaron Yang, Xiangxin Yang, Yen Ting Kuo, Sreeram Cingarapu, Dr.Kennedy Kalebaila – I will treasure our friendships forever and I will always be grateful for all of the help and guidance you have all given me.

To Biaobing Wang – thank you for your time and dedication. Your DSC and TGA analysis was vital to our work.

Finally, I would like to express my gratitude to both the Chemistry and Grain Science Departments here at Kansas State University for funding this research.

Dedication

For my family

CHAPTER 1 - Introduction

Petroleum, perhaps the most important commodity in the world, is the basis for the fuels and plastics we are all accustomed to and have come to rely on. However, in recent years, concerns regarding the renewability and rising costs of petroleum have become more insistent and as a result, bio-based fuels and plastics are receiving a great deal of attention, by both the media and the scientific community. Great strides have been made in the development of bio-fuels, as evidenced by the presence of E10 unleaded at most fueling stations. While the advances in the fuel industry are vital to our way of life, bio-plastics and biopolymers are also an important part of our everyday lives and as such, deserve an equal amount of attention.

Biopolymers are appealing for several reasons, one of which is that they are synthesized from oils obtained from renewable resources such as corn, sugar beets, and soybeans. Additionally, these crops are readily available, as 800 billion pounds are produced annually in the United States alone, only half of which is spoken for as food and feedstock, leaving nearly 400 billion pounds of grain available for harvesting the oils used in the production of biopolymers.[1] In addition, many bioplastics are biodegradable, making them ideal for disposable items such as plastic dishware, waste sacks, disposable gloves, mulching films, packaging materials, drug delivery aids, and suturing materials.[2] The final and most media-friendly advantage of biopolymers and plastics is the price; in the past, bio-based materials were more expensive to produce due to compatibility reasons, but as processing technology has advanced and both the monetary and environmental prices associated with the use of petroleum continue to rise, the appeal of bio-based materials will rise accordingly.

The advantages associated with the use of bio-based polymers and plastics are numerous, but it is important to note that there are still a few obstacles associated with biopolymers that must be overcome before bioplastics can compete with their petroleum-based counterparts. According to Wool et al, durability, compatibility, affordability, and sustainability are the primary concerns that must be addressed.[1] Sustainability seems to be a "no-brainer" as it was established previously that the starting materials used in biopolymer production are renewable, but this is only true as long as there is land available to grow them. Thus, sustainability is dependent upon the optimization of land use by the agricultural community. Chemists can play no role in this issue. However, in addressing the remaining issues of affordability, compatibility, and durability, chemists play and will continue to play a very important role.

1.1 Introduction to Nanoparticles

For many years, the addition of inorganic fillers has been the most widely used technique to address durability issues associated with not only bio-based materials, but also common polymers such as polypropylene and polyethylene. However, more recently, the addition of inorganic nanomaterials has become a promising technique in the quest for stronger polymers and plastics.

Perhaps it is best to begin by explaining why nanoparticles are different from their bulk materials. The size of a nanoparticle can be anywhere between 1-100 nm and in order for a material to be classified as "nano", it must have at least one dimension on the nanometer scale. Additionally, a nanoparticle can contain anywhere from 100 - 1 million atoms and can take on many different shapes including, but not limited to sheets, fibers, plates, discs, and needles, to name a few. The small sizes of these nanomaterials lead to vastly increased surface areas, which when combined with the various shapes and edges on the surface of the materials, leads to

properties that are very different from the properties of the bulk material. In addition, when the particles are consolidated into materials on the macroscale, unique properties are often the result.[3,4]

The prospect of creating new materials with unique properties is exciting and is an excellent advantage of using nanomaterials as polymer fillers. However, there is also another important advantage; because of the high surface areas and increased reactivity observed in nanomaterials, lower loadings of additives are necessary in order to observe the same enhancements seen in polymers with five times as much bulk-scale fillers.[5,6] Thus, the use of nanomaterials rather than the typical inorganic fillers leads not only to the production of a reinforced polymer which exhibits exceptional properties, but the lower loading percentages required also lead to lower production costs, as less filler material is used.

Many nanoparticles are currently available commercially, including metal oxide powders of titania (TiO_2), silica (SiO_2), magnesium oxide (MgO), and alumina (Al_2O_3), to name a few. Additionally, silver and gold nanoparticles, as well as several semiconductor particles can also be synthesized in the lab using various well-known techniques. Perhaps the most widely-known class of nanomaterial used in the polymer industry, however, are the nanoclays, which includes hydrotalcite, octasilicate, mica fluoride, and the most common, montmorillonite.[4]

1.2 Nanoclays as additives to polymers

Nanoclays are a popular choice for polymer fillers because they are inexpensive and readily available, chemically inert, stable, and transparent.[4,7] In addition, the sheet-like shape of most nanoclays provides a high aspect ratio, which maximizes the surface interaction between the clay and the given polymer. Many polymer-nanoclay composites have been synthesized with positive results, including polypropylene[8], polyethylene[9], polystyrene, polyimide[10], and polyacrylate[11]-

clay nanocomposites. Each showed increases in both strength and modulus, when compared with the original polymers. In addition to enhancing the strength of the polymers, the transparency of the final products, which is an important characteristic in plastics, was not affected by the addition of the clay.

While the advantages of using nanoclays are obvious, unfortunately there are drawbacks as well. Nanoclays are very difficult to disperse in a polymer matrix, as a result of their hydrophilicity; therefore it is necessary to modify the surface of the clays before they are incorporated into the polymer.[4] These treatments take time and often the effort to overcome the incompatibilities between the inorganic and organic surfaces far outweigh the enhancements that are achieved by using the clay in the first place.

1.3 Our Research

Supply and demand is a universal law of economics and it has become painfully clear that as the supply of petroleum dwindles, the price will consequently soar and as a result, the attainability of petroleum to the masses, whether in the form of fuel or plastic commodities, will be severely tested. In addition, the environmental effects of petroleum-use are becoming a hot issue and people are looking for ways to be environmentally friendly. It is for these reasons that the production of bio-based materials has gained so much attention in recent years. Numerous laboratory experiments have shown that additives are necessary in order for these materials to compete in today's market. In the past, nanoclays have been used extensively as additives in both petroleum and bio-based polymers and improvements in strength and modulus have been achieved in all cases. However, there are compatibility issues between the inorganic clay surfaces and the organic polymers in question. In our work, we intend to focus on the use of metal oxide nanoparticles as additives to the bio-based polymer, polylactic acid.

1.3.1 Introduction to polylactic acid

Polylactic acid (PLA) is a biodegradable thermoplastic which consists of aliphatic polyester units. PLA is typically synthesized via the ring opening polymerization (ROP) of lactide, shown schematically in Figure 1.1. This technique employs a tin catalyst, such as tin (II) chloride in order to achieve high molecular weight PLA. Polymers synthesized using this method typically exhibit glass transition temperatures between 50-80°C and melting temperatures between 173-178°C.[1]

Figure 1.1 Ring Opening Polymerization reaction of lactide to synthesize PLA

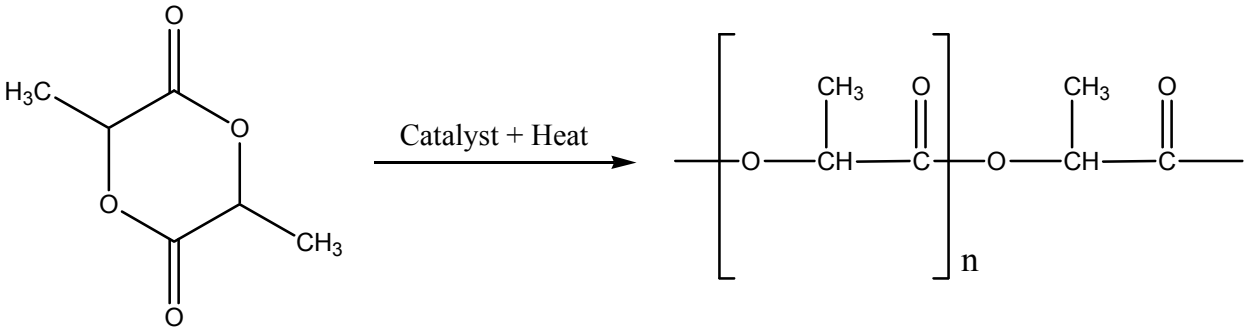

Lactide **Polylactic Acid**

While ROP may be the most accepted method, direct condensation of the lactic acid monomer, $C_3H_6O_3$, is also possible. Direct condensation involves heat treating the monomer under vacuum to form a prepolymer, which is then treated with the tin catalyst, referred to above, and then further heating is applied to produce high molecular weight PLA. The typical polymerization process is shown schematically in Figure 1.2.

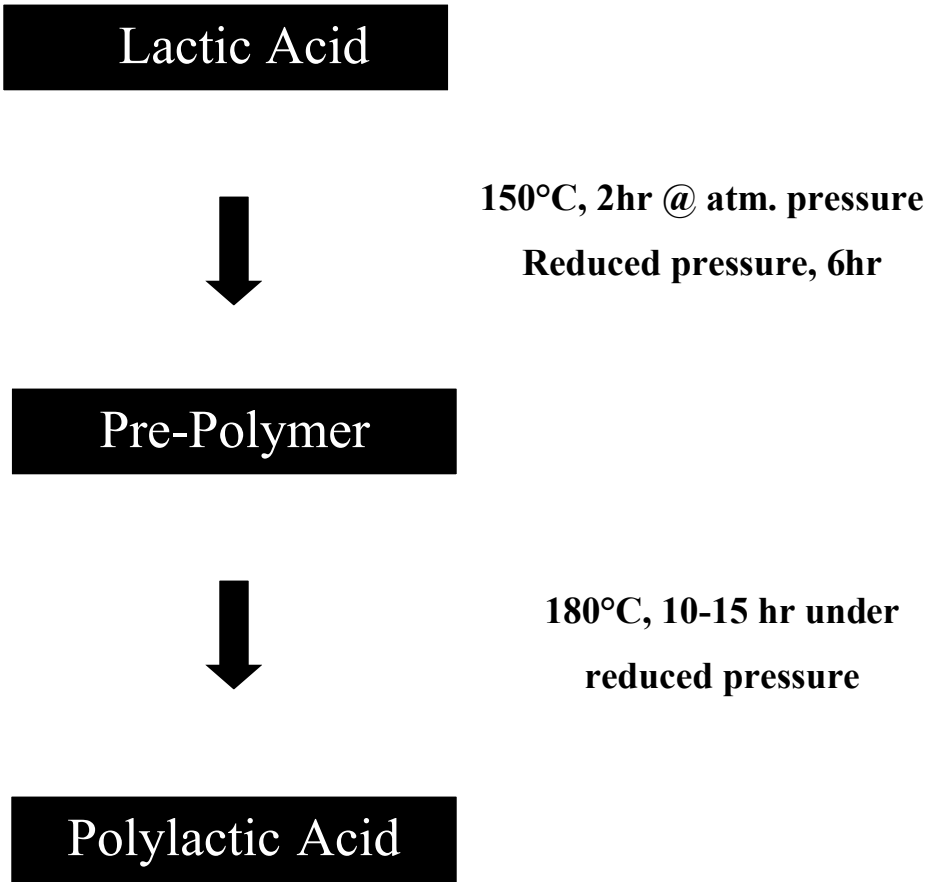

Figure 1.2 Procedure for direct condensation synthesis of PLA

Direct condensation produces high molecular weight PLA with the same melting and glass transition characteristics, as long as the reaction is conducted under good vacuum conditions. Water is formed as a byproduct of the reaction between the carboxylic and hydroxyl end groups, which can potentially result in hydrolysis of the newly formed ester connections, thus the vacuum treatment is necessary in order to remove the water before it can react with the newly formed polymer.

PLA is receiving a lot of attention from the plastics industry not only because it is an inherently biodegradable polymer, but also because it exhibits other desirable properties, such as

a clear and glossy surface, much like polypropylene, a significant resistance to both grease and moisture, as well as being an excellent barrier to both flavors and odors.[1] These characteristics are in high demand from bottling companies such as Pepsi® and Coca Cola®. However, PLA tends to lose its stiffness when it is heated above its glass transition temperature, thus the thermal stability of the polymer is lacking for these types of applications. Nevertheless, PLA has found numerous applications in the medical industry, including sutures, stints, and drug delivery devices.[12]

The overall focus of our work is to preserve the favorable properties of PLA, while increasing its thermal stability and durability by the addition of metal oxide nanoparticles. Magnesium oxide nanoparticles were chosen because they are environmentally friendly, well-characterized materials that due to their basicity, should not exhibit the compatibility issues associated with the use of nanoclays.

1.3.2 Magnesium oxide nanoparticles as additives to lactic acid

Magnesium oxide nanoparticles, as well as many of their potential applications, have been well characterized.[3] There are three different forms of magnesium oxide that can potentially be used as additives in the synthesis of stronger, more durable biopolymers: Commercial Magnesium Oxide (CM-MgO), Nanoactive® Magnesium Oxide (NA-MgO), and Nanoactive Magnesium Oxide Plus® (NA-MgO Plus) all of which are available commercially. In addition, magnesium oxide nanorods are also available via laboratory synthesis, but were not a focus of this study.[13]

Each of the three types of magnesium oxide used in our research differs in both surface area as well as morphology; CM-MgO has a cubic morphology and only 30 m^2/g surface area, while NA-MgO exhibits hexagonal morphology and a surface area of 250 m^2/g, and NA-MgO Plus

displays the highest surface area of the three with 750 m^2/g and a very unique fibrous morphology. Figure 1.3 summarizes the different shapes and sizes observed in magnesium oxide.

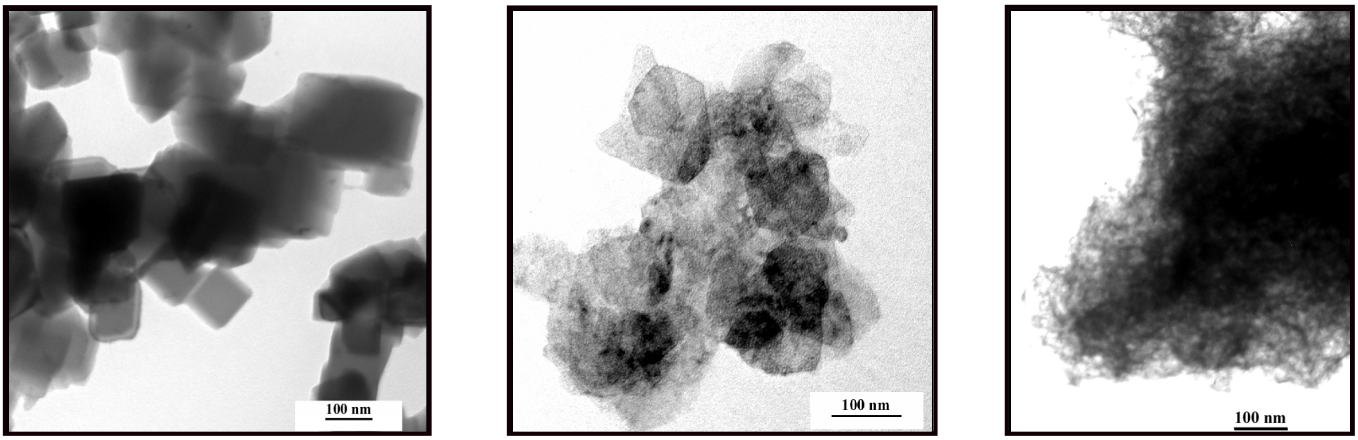

Commercial Magnesium Oxide	Nanoactive® Magnesium Oxide	Nanoactive MgO Plus®
Surface Area: 30m^2/g	Surface Area: 250m^2/g	Surface Area: 750m^2/g
Morphology: Cubic	Morphology: Hexagonal	Morphology: Fibrous

Figure 1.3 Magnesium oxide surface areas and morphologies

1.3.3 Possible Chemistry: Acid + MgO nanoparticles

As chemists, our primary goal is to identify how the different surface areas and morphologies of the MgO particles affect the polymerization and physical properties of the lactic acid polymers. In order to do this, each of the three MgO particles will be used as an additive in the direct condensation polymerization of lactic acid. Several possible pathways have been proposed for the reaction between lactic acid and magnesium oxide nanoparticles. The possibilities are as follows:

Acid-Base Reaction:

A likely reaction is that of an acid-base reaction, the product of which would be primarily unreacted lactic acid, as well as a small amount of magnesium lactate salt.

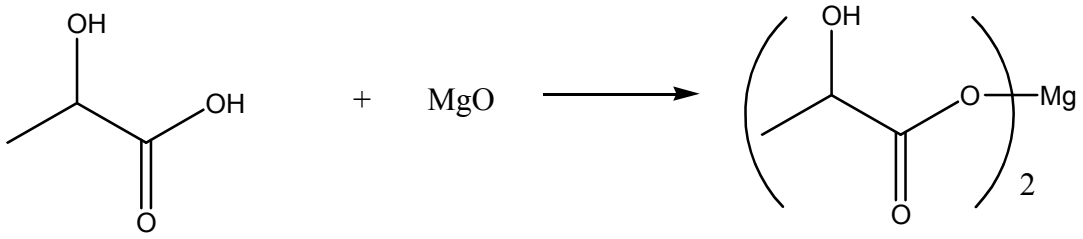

Polymerization Reaction (1):

Another possibility is that the acid functional groups of two lactic acid monomers react with each other to form an anhydride and then further polymerization is possible between other lactic acid monomers and the remaining hydroxyl functional groups. In this pathway, MgO could act either as a catalyst for the dehydration reaction or may merely be present as a filler material for the resulting polymer.

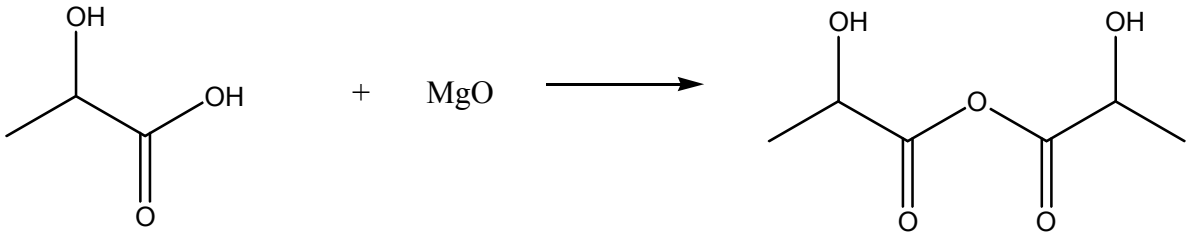

Polymerization Reaction (2):

This pathway involves two or more monomers reacting together to remove water and form straight-chain PLA. This is the most typical pathway for lactic acid to take when

polymerizing. In this case, MgO could again act as either a catalyst for further polymerization or may fill empty space in the matrix, resulting in a reinforced polymer.

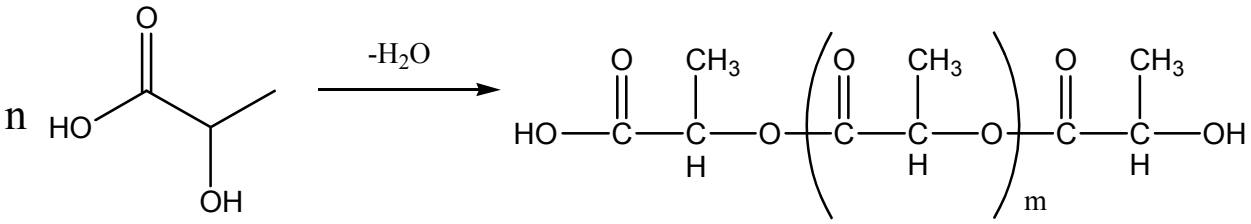

Polymerization Reaction (3):

In this reaction, the presence of MgO would catalyze the production of acrylic acid, followed by the addition of a lactic acid monomer across the double bond to form a polyester. The scheme below shows the addition of the monomer via the carboxylic acid protons, but the polymerization could also occur through the hydroxyl proton, which would produce a completely different polyester.

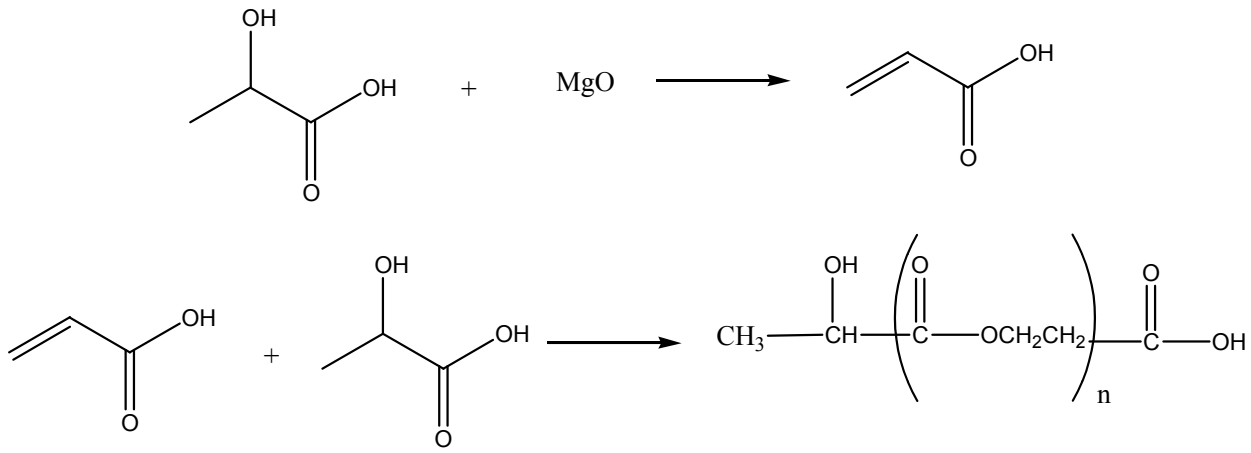

Polymerization Reaction (4):

It is also possible, that rather than acting as a catalyst or merely just a filler for the aforementioned polymerization reactions, the hydroxyl groups on the surface of the magnesium oxide particles may also chemically react with the lactic acid such that several different growing sites may be located on a given particle, as shown in Figure 1.4. If this is the case, the morphologies of the particles will play a significant role in the polymerization of the polymer.

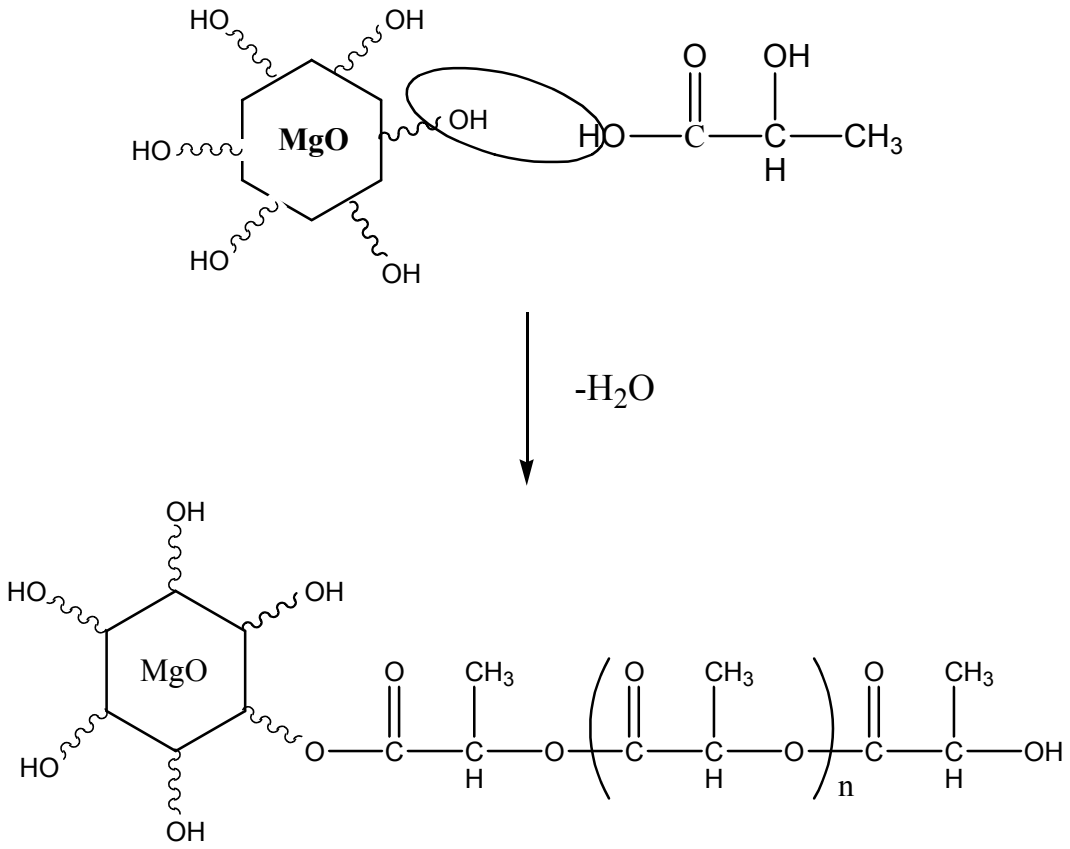

1.3.4 Methods of Analysis

In order to determine through which of these pathways the polymerization occurs, pre-polymer composites were synthesized and the structural differences were analyzed using FTIR, UV-Vis, ^{1}H and ^{13}C NMR, and TEM[14]. In addition, lactic acid titrations with each of the three types of magnesium oxide were performed in order to determine the effect of surface area on the observed equivalence points. Finally, the affect of the nanoparticles on the thermal and mechanical properties of the resulting polymer composites were studied using DSC and TGA.

CHAPTER 2 - Experimental Methods

2.1 Establishing a synthetic method

2.1.1 Initial synthesis of LA – MgO nanocomposites

Materials

A 90% aqueous solution of L(+)-Lactic Acid from Acros Organics, ACS grade magnesium oxide from Sigma Aldich as well as Nanoactive® and Nanoactive Plus® magnesium oxides from NanoScale Corporation were all used without further purification.

Synthesis

As very little work had been performed in this particular area of research in the past, it was necessary to make some preliminary observations regarding the nature of the reaction between lactic acid and each of the magnesium oxide materials. In order to do this, the two materials were mixed together in equimolar amounts with vigorous stirring. Each of the MgO materials formed a white, wax-like precipitate with the lactic acid monomer.

The effect of decreasing the amount of MgO material was also examined using this rudimentary synthetic method. The amount of MgO was cut by half and then mixed with the lactic acid monomer. In this case, a white precipitate formed as before, but the consistency of the product was more viscous than that of the previous samples.

TEM analysis of the samples indicated agglomeration of the particles was occurring, which resulted in poor mixing. In addition, polymerization is typically catalyzed by the application of heat, thus the room temperature environment in which the reaction took place

appeared to be hindering the polymerization of lactic acid. As a result, it became obvious that a high boiling point solvent was required in order to disperse the particles and provide the increased reaction temperature necessary to see polymerization.

2.1.2 Identifying an appropriate solvent

The choice of solvent was difficult as there were a number of stipulations that had to be met before a solvent could be chosen. The solubility of lactic acid and the dispersibility of the MgO particles in the solvent were the primary concerns, but it was also necessary to consider whether or not the solvent would participate in the reaction. THF, methanol, and ethanol were all identified as potential solvents, as lactic acid was highly soluble in all three. However, reactions between alcohols and carboxylic acids to produce ester functionalities are very common and as a result, THF was the frontrunner as it was the least likely to participate in the reaction. Unfortunately, magnesium oxide did not disperse well in the solvent, leaving the alcohols as the primary options. Ultimately, the best dispersion of magnesium oxide was achieved in methanol.

The amount of solvent was also important as the primary concern associated with the use of solvent is that it must be removed at the end of the reaction. In order to identify the best reaction conditions, the MgO particles were stirred in 50 mL and 100 mL aliquots of methanol and lactic acid was added after 30 minutes. The two were allowed to react for 2 hours and then the solvent was evaporated using a rotaevaporator. TEM images (Figures 1.5, 1.6, 1.7, and 1.8) were taken of the two products to analyze how the amount of solvent affected the dispersion of the particles within the polymer matrix. Additionally, the exact same reactions conditions were used to synthesize the products, with one exception; the solvent was heated to its boiling point, ~60°C, and the reaction was carried out at elevated temperatures. TEM images (Figures 1.5, 1.6,

1.7, and 1.8) were taken to identify how temperature affected the dispersion of the particles and polymerization of lactic acid.

2.1.3 Titrimetric analysis of MgO particle consumption by lactic acid

As was mentioned in the introduction, the most obvious reaction that might occur between lactic acid and magnesium oxide is that of an acid-base neutralization where the lactic acid consumes the particles rather than reacting with the surface. Once an appropriate solvent had been determined, an acid-base titration was performed in hopes of determining how the reaction differs with the three diverse particles; if the particles are being consumed in an acid-base reaction, the equivalence points should be the same, while if the surface area and/or shapes of the different particles have an effect on the reaction pathway, the equivalence points should differ.

The titrations were carried out by first dissolving 2 grams (0.02 mol) lactic acid in 100 mL methanol. One gram of each of the three types of magnesium oxide was added gradually to the vigorously stirring lactic acid/methanol solution. pH measurements were recorded after each addition and a titration curve was created for each sample (Figure 3.6). An equivalence point of 0.45g (0.01 mol) was expected, but instead, a steady increase in the equivalence points with increasing surface area of MgO material was observed. The equivalence points for each sample were as follows: LA w/ CM-MgO, 0.360g; LA w/ NA-MgO, 0.455g; LA w/ NA-MgO Plus, 0.499g.

2.2 Synthesis and characterization of LA – MgO nanocomposites in methanol

2.2.1 Synthesis of Lactic Acid – MgO nanocomposites in methanol

Materials

A 90% aqueous solution of L(+)-Lactic Acid from Acros Organics, ACS grade magnesium oxide from Sigma Aldich as well as Nanoactive® and Nanoactive Plus® magnesium oxides from Nanoscale Materials, and ACS grade methanol from Fisher Scientific, were all used without further purification.

Synthesis

Lactic acid – magnesium oxide composites were synthesized in methanol with 18%, 10%, 5%, and 1% by weight loadings of each of the three magnesium oxide materials mentioned above. To begin, the appropriate mass [18% loading: 0.45g (11mmol), 10% loading: 0.22g (5.5mmol), 5% loading: 0.11g (2.7mmol), 1% loading: 0.03g (0.7mmol)] of MgO particles were suspended in 100 mL of methanol. The mixture was allowed to reflux, with vigorous stirring for 30 minutes at approximately 65°C, in order to achieve adequate dispersion of the particles. Approximately two grams (22 mmol) of lactic acid were added and allowed to react with the suspended particles for 2½ hours. A white precipitate formed upon the addition of lactic acid to each of the three types of MgO. The precipitate formed immediately with commercial MgO and more gradually with the nanoactive samples. Upon completion of the reaction, excess methanol was removed using a rotoevaporator. The product was heat treated at 60°C (Ramp time: 1 hour, Soak time: 2 hours) under vacuum and then left under vacuum overnight in order to remove any trace amounts of solvent from the final product. After drying, the products were collected as

solids in the cases with higher loadings and semi-solids in the cases with the lowest loading (1%).

2.2.2 Thermal analysis of composites

In order to assess the amount of solvent remaining after the heat treatment under vacuum, thermogravimetric analysis was performed using a Shimadzu TGA-50 on the samples before and after drying under vacuum. Approximately 15 mg of each sample was heated under a steady flow of helium from room temperature to 500°C at 10°C/min in a platinum pan. TA-60 software was used to analyze the weight loss data.

Weight losses of between 50-60% were observed upon heating from room temperature to 200°C, indicating the presence of an immense amount of solvent in the samples before being placed under vacuum. Additionally, methyl esters, formed via the side reaction of lactic acid and methanol may also have contributed to the weight loss observed in this temperature range.

Upon heating under vacuum at 60°C, a significant decrease in the weight lost below 200°C was observed, as weight losses between 10-15% were observed. This indicates that the majority of solvent was removed by the heat treatment under vacuum, which was also confirmed via visual inspection of the samples. Any lingering solvent was not expected to interfere with further analysis of the samples. The remaining percentage of weight lost is likely due to the presence of the methyl ester groups mentioned previously.

2.2.3 Structural characterization via infrared analysis

Approximately 2 mg of each of the final products (after heat treatment at 60°C) were ground together with potassium bromide until a fine powder was achieved. The powder was formed into a pellet and analyzed using a Nexus 670 FTIR spectrophotometer. In the samples where the consistency of the final product was more like a semi-solid, a KBr pellet was prepared

as above and then a thin layer of the product was applied to the pellet for analysis. The peaks observed for each sample, along with their relative intensities are summarized in Table 2.1.

According to Silverstein et al[14], the following peak assignments can be made from the data: Broad peaks at ~3000 cm^{-1} are likely a combination of the hydroxyl functional groups of the lactic acid polymer as well as the surface hydroxyl groups of the magnesium oxide particles. Additionally, trace amounts of water may also be present as a bi-product of the condensation process. The peaks between 1730-1740 cm^{-1} can be attributed to remaining carboxylic acid functionalities from the lactic acid monomers or from newly formed ester functional groups, both of which may be present in the samples. The presence of carboxylate ions result in the peaks between 1600-1615 cm^{-1} and 1430 cm^{-1}. Finally, further evidence of polymerization is provided by the ester peaks at 1200 and 1120 cm^{-1}.

Table 1.1: Summary of infrared peaks for LA-MgO composites prepared in MeOH

Sample	Peak frequency (cm^{-1})
LA : CM-MgO, 18% loading	3200(s, broad), 1740(m), 1613(s), 1432(m), 1282(m), 1121(s)
LA : NA-MgO, 18% loading	3360(s, broad), 1603(s), 1429(m), 1282(m), 1121(s)
LA : NA-MgO Plus, 18% loading	3377(s, broad), 1733(m), 1617(s), 1419(m), 1278(m), 1124(m)
LA : CM-MgO, 10% loading	3360(s, broad), 1742(m), 1683(s), 1431(m), 1281(m), 1122(s)
LA : NA-MgO, 10% loading	3349(s, broad), 1743(w), 1683(s), 1431(m), 1281(m), 1122(s)
LA : NA-MgO Plus, 10% loading	3342(s, broad), 1733(w), 1650(s), 1431(m), 1278(m), 1122(s)

Table 1.1, cont'd

LA : CM-MgO, 5% loading	3358(s, broad), 1739(m), 1626(s), 1431(m), 1281(m), 1122(s)
LA : NA-MgO, 5% loading	3356(s, broad), 1739(m), 1626(s), 1431(m), 1281(m), 1122(s)
LA : NA-MgO Plus, 5% loading	3142(s, broad), 1739(m), 1615(s), 1430(m), 1280(m), 1122(s)
LA : CM-MgO, 1% loading	2984(m, broad), 1719(s), 1626(w), 1454(m), 1373(m), 1205(s), 1123(s)
LA : NA-MgO, 1% loading	2984(m, broad), 1719(s), 1626(w), 1454(m), 1373(m), 1205(s), 1123(s)
LA : NA-MgO Plus, 1% loading	2984(m, broad), 1719(s), 1626(w), 1454(w), 1369(w), 1213(s), 1127(s)

2.2.4 Transmission Electron Microscopy analysis

A vital component of this research is identifying the differences that occur as a result of adding magnesium oxide nanoparticles with different shapes and sizes to the biopolymer, (poly)lactic acid. A transmission electron microscope was employed in hopes of viewing the differences in the physical structures of the resulting nanocomposites.

Preparing the samples for TEM analysis involved sonicating each sample in ethanol for three minutes, the result of which was a complete suspension of the product in the solvent. The product was allowed to settle for approximately 30 minutes and then a drop of the dilute suspension was placed onto a carbon-coated copper grid. Solvent was evaporated from the grid, leaving a thin-layer of product on each grid.

TEM analysis was performed using a Philips CM 100 Transmission Electron Microscope (Biology Department, Kansas State University). Liquid nitrogen cooling was necessary to prevent decomposition of the samples under the high vacuum and electron beam environment of the TEM. TEM analysis was conducted on each of the following samples: LA w/ CM-MgO, LA w/ NA-MgO, and LA w/ NA-MgO Plus at 18%, 10%, 5%, and 1% loadings of magnesium oxide. Initial results indicated that the samples with lower loadings were more promising than those with higher loadings.

2.3 Synthesis and characterization of LA – MgO nanocomposites in propanol

2.3.1 Synthesis of Lactic Acid – MgO nanocomposites in propanol

Materials

A 90% aqueous solution of the monomer, L(+)-Lactic Acid from Acros Organics, ACS grade magnesium oxide from Sigma Aldich as well as Nanoactive® and Nanoactive Plus® magnesium oxides from Nanoscale Materials, and ACS grade propanol from Fisher Scientific, were all used without further purification.

Synthesis

From the TEM and IR analysis of the samples prepared in methanol, it became obvious that lower loadings of magnesium oxide and higher reaction temperatures were required in order for polymerization to occur, thus the composites were synthesized in propanol with 1% by weight loadings of each of the three types of magnesium oxide. Additionally, it became obvious that a scale-up of the synthesis was necessary in order to produce enough sample for the various measurements required to adequately characterize the composites.

A 5X scale-up was achieved by using 10 grams (110 mmol) of lactic acid and ~0.15 grams (3.7 mmol) MgO in 150 mL of propanol. The particles were suspended in propanol and the mixture was allowed to reflux, with vigorous stirring for 30 minutes at ~110°C, in order to achieve adequate dispersion of the particles. The lactic acid was added and allowed to react with the suspended particles for 2½ hours. A white precipitate formed upon the addition of lactic acid to each of the three types of MgO. After the reaction was complete, excess propanol was decanted and then the remaining propanol was removed using a rotoevaporator. The product was then placed under vacuum overnight and a heat treatment of 100°C (Ramp time: 2 hours, Soak time: 2 hours) was applied in order to remove excess solvent from the final product. After drying, the products were collected in the form of semi-solids.

A prepolymer control was also synthesized using the same procedure; propanol was refluxed for 30 minutes (without MgO) and then 10 grams lactic acid was added and allowed to react for 2½ hours. Excess solvent was decanted as before and remaining solvent was removed using a rotaevaporator. The sample was dried under vacuum with a 100°C heat treatment for 2 hours. Finally, the sample was left under vacuum overnight to remove as much propanol as possible. The final product was collected as a clear liquid.

2.3.2 Structural characterization via IR analysis

Potassium bromide was ground into a fine powder and transparent pellets were prepared using a pellet press. A thin layer of the final products was applied to the pellets and analysis was conducted using a Nexus 670 FTIR spectrophotometer. The peaks observed for each sample, along with their intensities are summarized in Table 2.2.

Table 2.2 Summary of infrared peaks for LA-MgO composites prepared in propanol

Sample	Peak frequency (cm^{-1})
LA pre-polymer	3300(m, broad), 1735(s), 1454(m), 1212(m), 1127(s)
LA : CM-MgO, 1% loading	3300(s, broad), 1735(s), 1591(s), 1462(w), 1279(m), 1116(s)
LA : NA-MgO, 1% loading	3300(s, broad), 1731(s), 1475(w), 1373(w), 1209(s), 1123(s)
LA : NA-MgO Plus, 1% loading	3300(s, broad), 1723(s), 1454(w), 1365(w), 1205(m), 1116(s)

Many of the peaks in the samples prepared in propanol are similar to those observed in the samples prepared in methanol. The broad peaks at 3300 cm^{-1} are due primarily to the hydroxyl groups of the polymer as well as hydroxyl groups on the surface of the magnesium oxide particles. As before, water may also play a slight role in the broadness of this peak. The peaks at ~1730, 1200, and 1120 cm^{-1} are due to ester functionalities, indicating polymerization has occurred. Finally, the peaks at 1591 and between 1450-1462 cm^{-1} are due to the presence of carboxylate ions.

2.3.3 Structural characterization via NMR analysis

^{1}H and ^{13}C NMR in d_6-DMSO were performed on each of the products synthesized in propanol using a Varian Unity 400MHz NMR. Spectra were reported in ppm and the composite spectra are shown in Figures 3.14 and 3.15.

2.2.4 Structural characterization via TEM

Each of the four samples prepared in propanol were sonicated in ethanol for three minutes, the result of which was a complete suspension of the product in the solvent. The product was allowed to settle for approximately 30 minutes and then a drop of the dilute suspension was placed onto a carbon-coated copper grid. The solvent was allowed to evaporate from the grid, leaving a thin-layer of each of the products on the grid.

TEM analysis was performed using a Philips CM 100 Transmission Electron Microscope (Biology Department, Kansas State University). Liquid nitrogen was utilized to prevent decomposition of the samples as a result of the high vacuum and electron beam environment. TEM analysis was conducted on each of the following samples: LA w/ CM-MgO, LA w/ NA-MgO, and LA w/ NA-MgO Plus, all with 1% loadings of magnesium oxide. Unfortunately, an adequate picture of the prepolymer control was not acquired, as the sample consistency was not conducive to TEM imaging.

2.3.5 UV-Vis analysis of composites

Each of the composites, along with the prepolymer control and the lactic acid monomer starting material were analyzed via UV-Vis spectroscopy. A Varian UV-Vis-NIR spectrophotometer was employed for the analysis. Each of the samples was dissolved in DMSO and a scan from 200-800 nm was performed. Origin software was used to prepare a plot of the resulting data (Figure 3.19)

The plot shows a slight change in the absorption maximum in each of the samples. The LA monomer shows a λ_{max} of ~290 nm, while λ_{max} values for the composites are as follows: the CM-MgO sample shows a red shifted peak with an additional shoulder (λ_{max} = 255 nm, shoulder

@ 290 nm), a red shifted, broadened peak for the NA-MgO sample (λ_{max} = 260 nm), and a slightly red shifted, symmetrical peak for the NA-MgO Plus sample (λ_{max} = 280 nm).

2.3.6 Thermal analysis of composites via TGA and DSC analysis

2.3.6.1 Melting Properties

Differential scanning calorimetry (DSC) was used to characterize the melting properties, including melting temperature, melting enthalpy, and glass transition temperatures for each of the aforementioned nanocomposites. A Perkin-Elmer Pyris 1 calorimeter was used in the analysis. The DSC was calibrated with an indium standard and all experiments were performed under a constant flow of nitrogen.

For the sample analysis, approximately 3-4 mg of dried sample was sealed in an aluminum DSC pan for analysis. After holding for 1.0 minute at 30°C, the sample was heated to 170°C at a rate of 10°C/min and then held at this temperature for three minutes in order to eliminate any previous thermal history. The sample was then cooled to -20°C at -100°C/min and held at -100°C for three minutes. Finally, the sample was heated to 170°C at 10°C/min again. Both the first and second heat scans were recorded. Peak temperatures were used to identify both melting and cold crystallization temperatures and peak areas were to calculate melting enthalpies for each of the samples. The results of this study are summarized in Figure 3.20 in Chapter 3.

2.3.6.2 Thermal Stability

The thermal stability of each of the composites was evaluated using a Shimadzu TGA-50. A constant flow of nitrogen was applied while heating the samples from 50-800°C at a rate of 10°C/min. Commerical, Nanoactive®, and Nanoactive Mgo Plus® were also measured as

controls. The results of the thermal stability study are summarized in Table 3.1 and Figure 3.21 both of which can be found in Chapter 3.

CHAPTER 3 - Results and Discussion

(Poly)lactic acid is a very important industrial commodity in its own right, as it has found numerous applications in the medical field.[1] However, producers of PLA hope to market the polymer to the plastics industry, as PLA exhibits many properties that are desirable in plastics, such as a clear and glossy surface and a strong resistance to both moisture and odors. Unfortunately, PLA is unable to compete with popular polymers like polypropylene and polyethylene due to its lack of durability when heated above its glass transition temperature. Our research focuses on increasing the thermal stability and durability of PLA through the addition of metal oxide nanoparticles.

3.1 Establishing a synthetic method

Initially, several preliminary investigations were carried out in order to characterize how magnesium oxide nanoparticles would react with the monomer, lactic acid. At the outset, lactic acid and magnesium oxide (CM, NA, NA-Plus) were mixed in equimolar amounts, the result of which was a white, wax-like precipitate. No heat evolution was observed during the reaction, indicating that the acid-base reaction discussed in the introduction was not the primary reaction between the two. Additionally, it appeared that the amount of MgO added hindered the dispersion of the solid throughout the monomer, thus the amount was decreased and the product re-examined.

Decreasing the amount of MgO by half appeared to aid in mixing, as a more uniform semi-solid was produced. The product was much more viscous than the previous sample, but still showed small clumps of aggregated solid. In order to get a better picture of the interactions between the two, each of the samples was studied under the TEM (Figure 1.4).

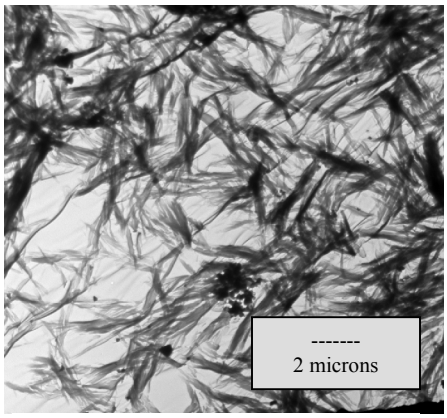

LA w/ CM-MgO

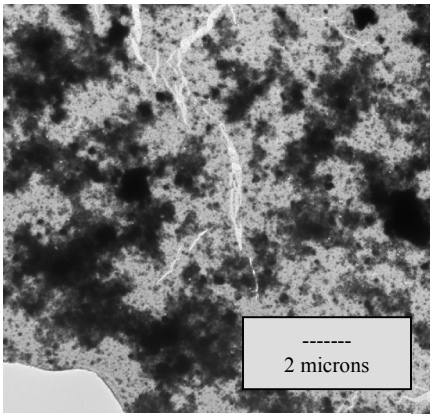

LA w/ NA-MgO

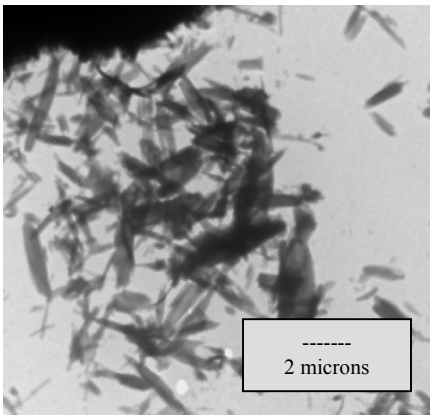

LA w/ NA-MgO Plus

Figure 1.4 Product of mixing lactic acid and magnesium oxide (18% loading)

It appears that a small degree of polymerization may have occurred in the samples with CM and NA-MgO Plus, as there is evidence of strand-like materials in both samples. However, agglomeration of the MgO particles appears to be a problem in all three samples, but especially

in the sample with NA-MgO. Very little polymer was observed in this sample; rather clumps of particles covered the majority of the grid. It appears from this analysis that very poor mixing was achieved by mixing the two starting materials directly. The poor mixing of the reactants results not only in agglomeration of the products, but also poor polymerization of the monomer. As a result, the need for a solvent was identified; dispersing the particles in solvent before mixing with the lactic acid would bring about better mixing and the high temperature environment would initiate polymerization of the monomer.

3.2 How does the amount of solvent and the reaction temperature affect the composite?

Methanol was identified as an appropriate solvent as lactic acid showed high solubility and the MgO particles dispersed well in the environment. However, the amount of solvent to use was still in question. In order to solve this dilemma, the composites were synthesized in 50mL and 100mL aliquots of methanol, with and without the application of heat. Excess solvent was evaporated using a rotoevaporator and then TEM images (Figures 1.5 and 1.6) were taken of each sample in order to identify how the amount of solvent and the application of heat affected the outcome of the final products.

From the TEM images of the composites with CM-MgO, it was obvious that 50mL of methanol was not enough to achieve adequate dispersion of the MgO particles, as the existing materials appear very dark, with very few interesting features. In contrast, the products synthesized in 100mL methanol have more contrast under the microscope. In addition, it was obvious that temperature had an affect on the reaction, but it was still unclear if the application of heat was favorable, thus the remaining composites were synthesized in 100mL methanol with

and without the application of heat and TEM imaging was conducted in order to better understand the influence of temperature on the reaction (Figures 1.7 and 1.8).

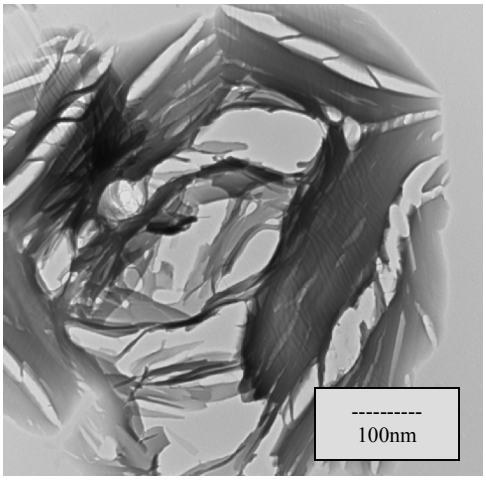

LA w/ CM-MgO
In 50mL MeOH

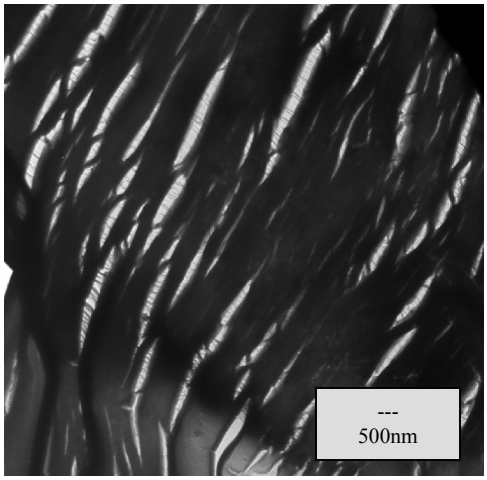

LA w/ CM-MgO
In 50mL MeOH + heat

Figure 1.5 Products of LA with CM-MgO in 50mL MeOH, with and without the application of heat

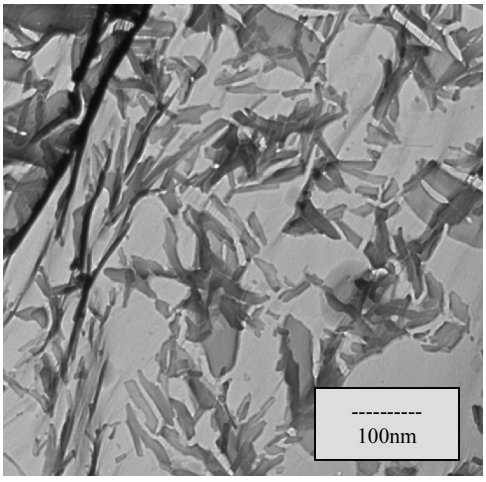

LA w/ CM-MgO
In 100mL MeOH

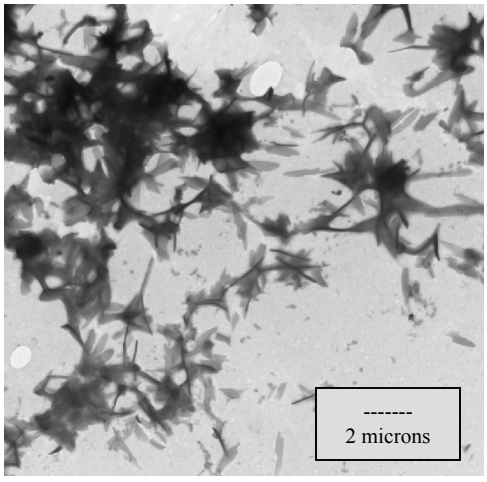

LA w/ CM-MgO
In 100mL MeOH + heat

LA with CM-M

hout the applica

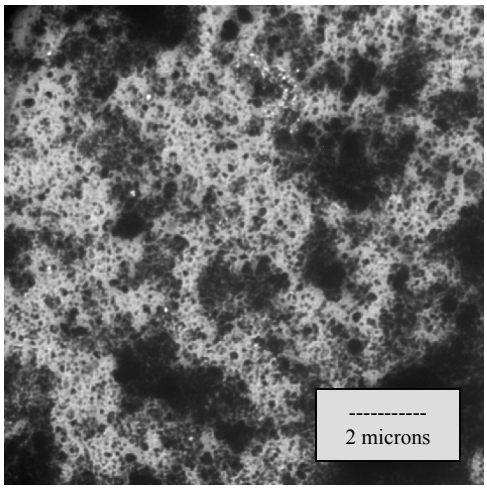

LA w/ NA-MgO
In 100mL MeOH

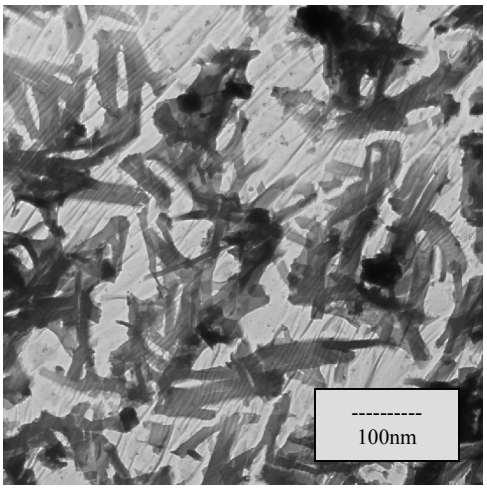

LA w/ NA-MgO
In 100mL MeOH + heat

LA w/ NA-MgO in 100

without the application of heat

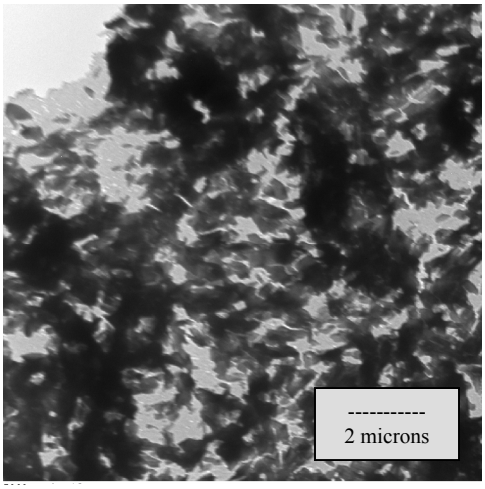

LA w/ NA-MgO Plus
In 100mL MeOH

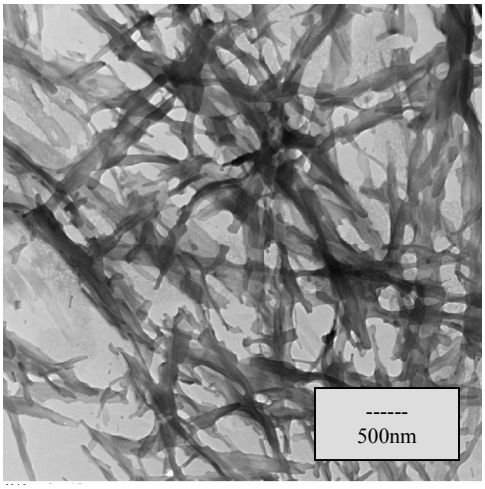

LA w/ NA-MgO Plus
In 100mL MeOH + heat

Figure 1.8 Product of LA w/ NA-MgO Plus in 100mL MeOH with and without the application of heat

The TEM images indicate that higher reaction temperatures are conducive to better dispersion of nanoparticles throughout the polymer matrix, as well as an increased rate of polymerization. In figures 1.7 and 1.8, significant agglomeration of the particles is shown in the products synthesized without heat, while in contrast, the products synthesized at higher temperatures show evidence of polymerization and a lack of particle accumulation. Therefore, the standard synthetic method was established: disperse particles in refluxing methanol for approximately 30 minutes to attain maximum dispersion of the nanoparticles, followed by the addition of lactic acid. In order to synthesize a mid-molecular weight prepolymer, optimum reaction time was determined to be 2½ hours. Excess solvent will be removed via decanting and evaporation under vacuum.

3.3 Is lactic acid consuming the MgO particles?

It is vital to our research that either the size and/or the shape differences in the three types of magnesium oxide have an effect on the physical and chemical characteristics of the resulting PLA composite, thus we were very interested in establishing whether or not lactic acid merely consumed the particles upon addition or if the monomer was reacting with the unique surfaces of the different particles. In order to ascertain this information, titrations were performed assuming that if the particles were being consumed by lactic acid, the equivalence points of each titration would be identical, as surface area and/or shape would not have any effect if this was the case. In contrast, if lactic acid reacts with the surface of the particles, the surface areas will significantly alter the observed equivalence points.

Titrations were performed by dissolving lactic acid in methanol and then measuring the pH as each of the three MgO materials was added. Titration curves were created using Origin software (Figure 1.9). A steady increase in the equivalence points was observed as the surface

area of the MgO particles increased indicating that surface area *is* a factor in the reaction between lactic acid and the Nanoactive® magnesium oxides.

From the equivalence point masses and the known amount of lactic acid in the sample, it was possible to back-calculate the amount of lactic acid neutralized by each sample of magnesium oxide: CM-MgO:2.26 mol, NA-MgO:2 mol, NA-MgO Plus: 1.79 mol. These values illustrate that the commercial sample neutralized the most lactic acid with the least amount of MgO, indicating that the primary reaction between lactic acid and CM-MgO is an acid-base neutralization, whereas with the nanoactive samples, more material was required to reach the equivalence point and less lactic acid was neutralized, confirming that while the reaction exhibits some acid-base characteristics, surface reactions are occurring as well. It can be concluded that the larger, less reactive CM-MgO particles reacted more by acid-base neutralization and less by nanoparticles induced polymerization.

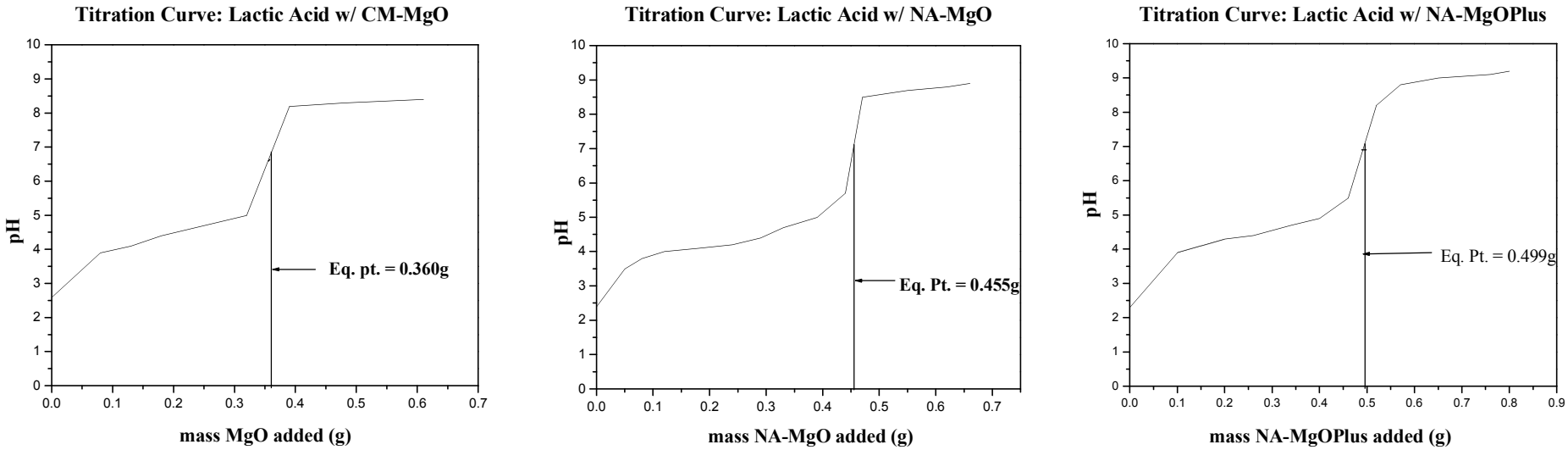

Figure 1.9 Titration curves for lactic acid with CM, NA, and NA-Plus MgO

3.4 Characterization of LA-MgO nanocomposites prepared in methanol

3.4.1 Infrared analysis of composites

Infrared analysis was performed on each of the following: LA w/ CM-MgO, LA w/ NA-MgO, and LA w/ NA-MgO Plus, each with 18%, 10%, 5%, and 1% by weight loadings of magnesium oxide. The primary peaks observed were: strong, broad peaks around 3000 cm^{-1}, attributed to the presence of the hydroxyl functional groups of the lactic acid polymer as well as a small contribution from the water produced as a bi-product of the condensation reaction; sharp peaks around 1730 cm^{-1} were also observed, indicating the presence of acid or ester functionalities from the lactic acid monomer or the newly formed ester linkages of the growing polymer; strong signals at 1615 and 1430 cm^{-1} established that carboxylate ions were a significant product of the reaction; and finally, peaks were observed between 1200-1100 cm^{-1}, confirming the presence of ester functionalities. Table 1.1 summarizes the peaks observed for each sample.[14]

All of the peaks mentioned above are present in each of the samples, regardless of the MgO loading. However, an interesting trend developed as the amount of MgO was decreased in the samples; the carboxylate signals at 1615 and 1430 cm^{-1} decreased in intensity, while the ester signals between 1200-1100 cm^{-1} increased in intensity, indicating that lower loadings of magnesium oxide led to improved polymerization. Additionally, in the products with 1% loadings of MgO, surface area appeared to have an affect on the polymerization of lactic acid, as the samples with Nanoactive® MgO showed weaker carboxylate signals than the samples with commercial MgO (Figures 1.10, 1.11, and 1.12), indicating the primary product in the nanocomposites was a polymer with multiple ester linkages, rather than a carboxylate salt, which appears to be the primary product of the reaction with the commercial sample.

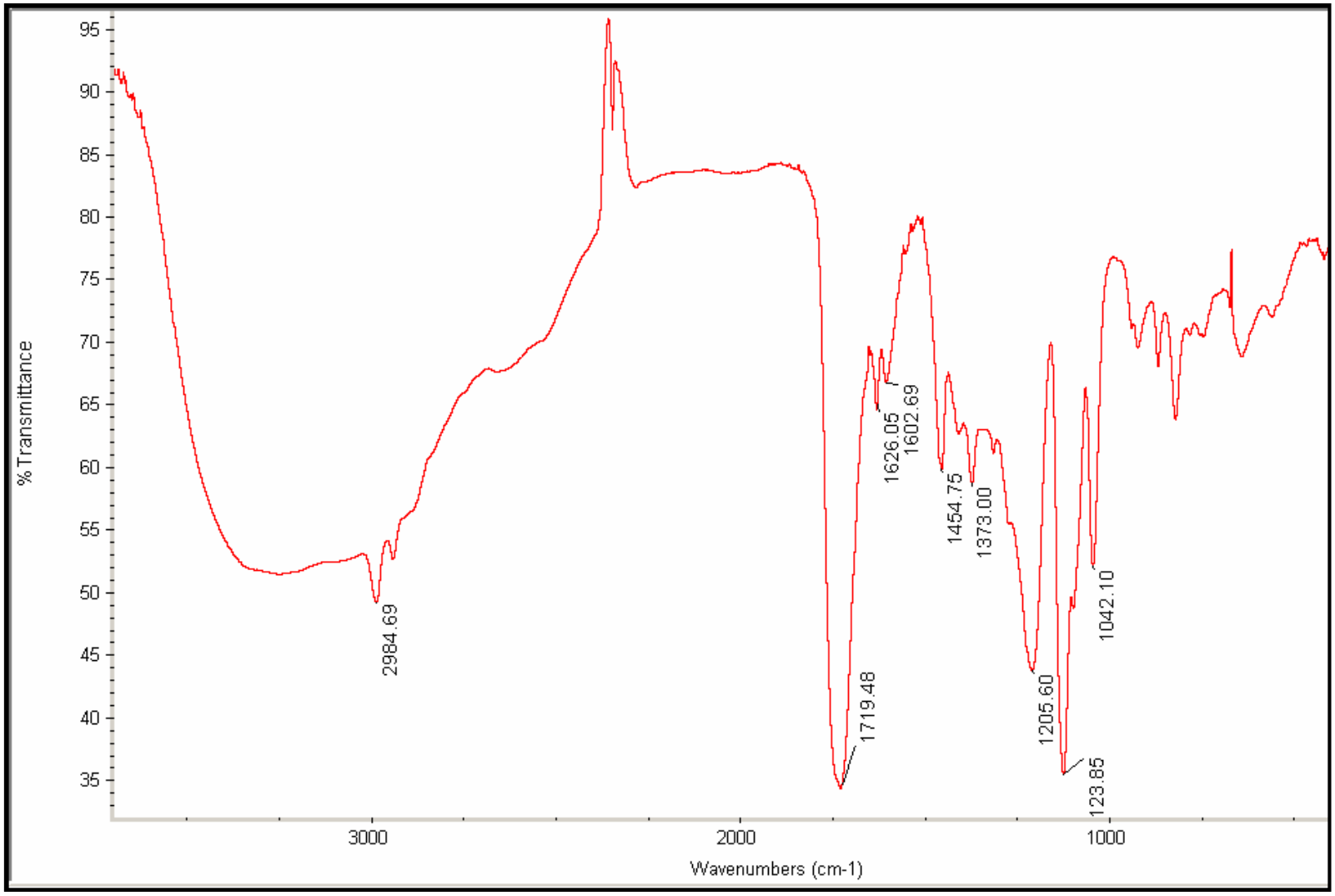

Figure 1.10 Infrared spectra of LA w/ CM-MgO (1% loading of MgO)

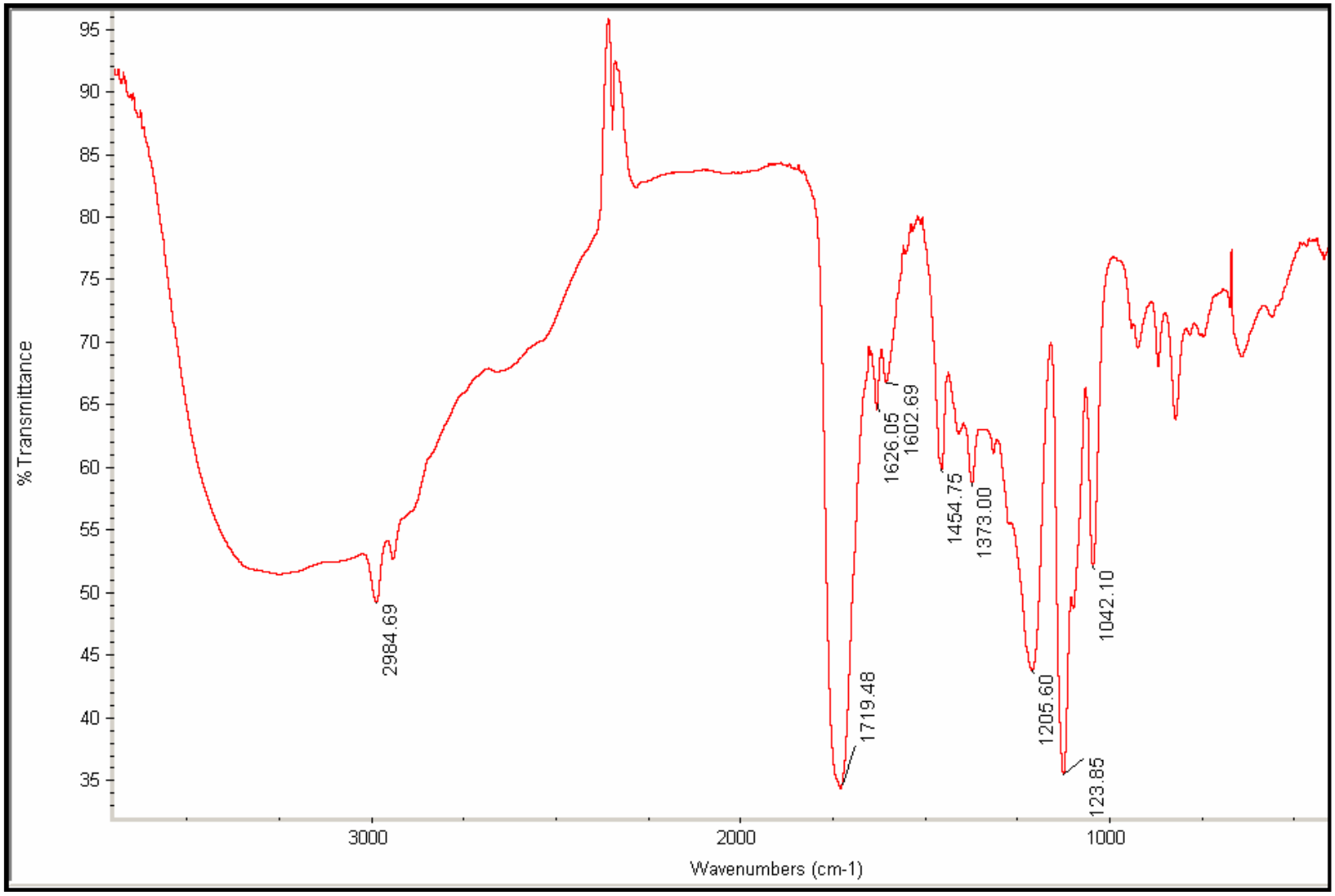

Figure 1.11 Infrared spectra of LA w/ NA-MgO (1% loading of MgO)

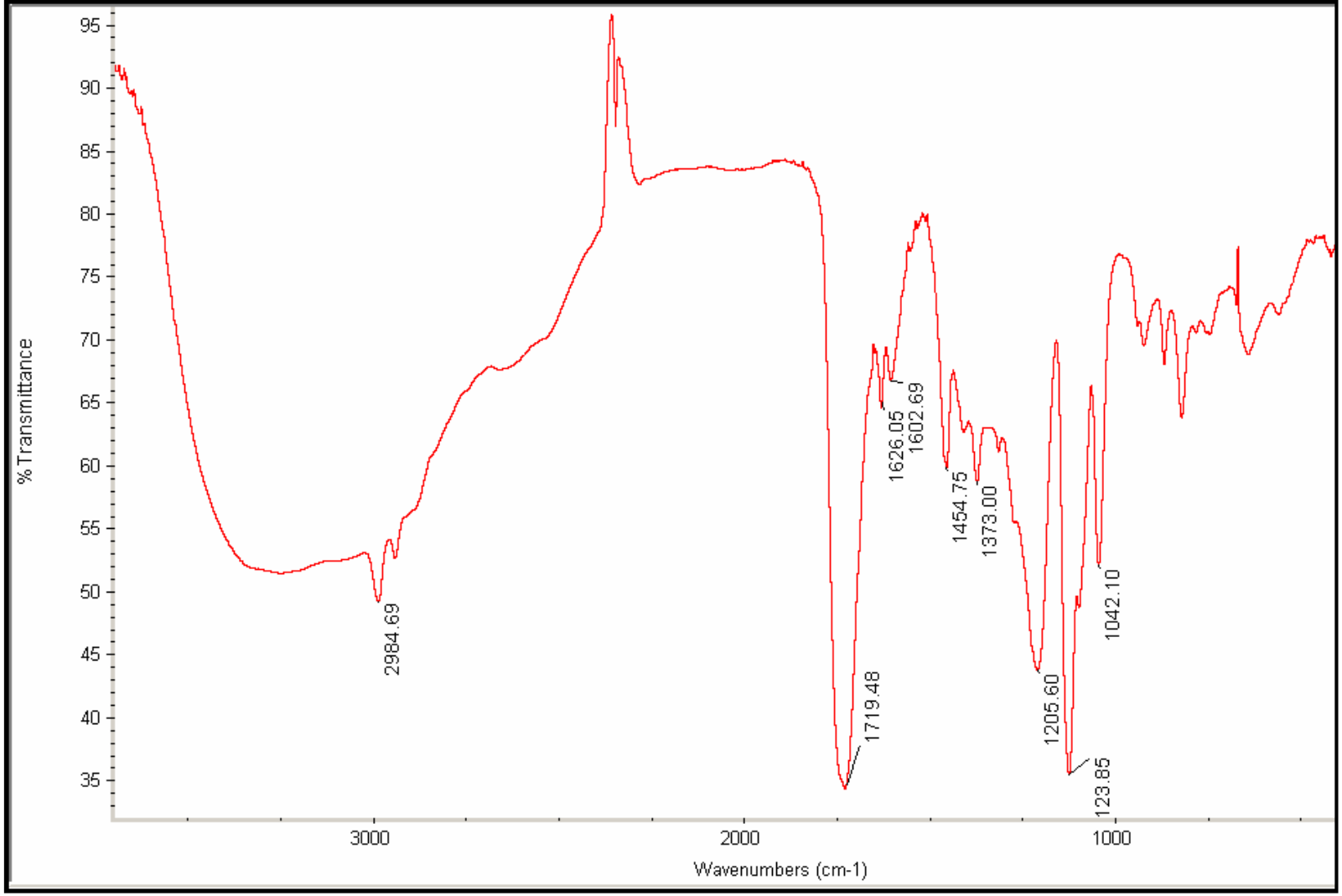

Figure 1.12 Infrared spectra of LA w/ NA-MgO Plus (1% loading of MgO)

3.4.2 TEM analysis of composites

Infrared analysis showed that there were slight differences in the chemistry of the three composites, but it was still unclear how these chemical differences affected the physical structures of the products, as their consistencies were very similar. In hopes of identifying further differences in the three composites, each was examined under a transmission electron microscope. Very little detail was observed in the samples with higher loadings, as most of the solids were clustered together much like the materials shown in figures 1.5, 1.6, and 1.7. However, the samples with 1% loadings of MgO turned out to be very interesting. Figures 1.13 and 1.14 show that the small chemical differences indicated in the infrared analysis led to immense structural differences.

Very little polymerization occurred in the reaction between lactic acid and commercial MgO, as only short, thick structures were observed under the microscope, which appears to confirm the results of the infrared study and the titration results. Therefore, the primary reaction between lactic acid and commercial MgO is an acid-base neutralization, the product of which is a carboxylate salt. However, some degree of polymerization does occur as polymer material was observed under the microscope and ester signals were evident in the infrared analysis, indicating that while commercial MgO does not catalyze polymerization, it does not hinder it either. Instead, magnesium oxide neutralizes the available lactic acid and then the remaining acid is polymerized via the application of heat. Polymerization *is* stunted however, as evidenced by the numerous, short polymer units, which indicates that polymerization was initiated and terminated many times.

In contrast, the size and/or shape of Nanoactive® MgO seems to be conducive to the polymerization of lactic acid, as a very unique structure featuring long, interconnected polymer

strands that exhibit a large degree of crosslinking was observed under the microscope for the sample containing NA-MgO. The unique structure along with the evidence for further esterification provided by the IR analysis points toward the fact that either surface area or the difference in shape or maybe even both, effects the polymerization of lactic acid.

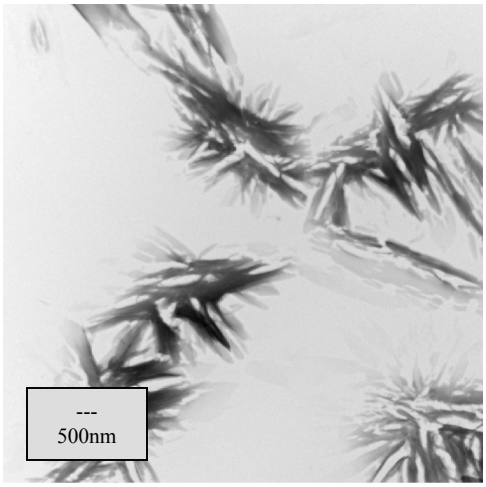

LA w/ CM-MgO

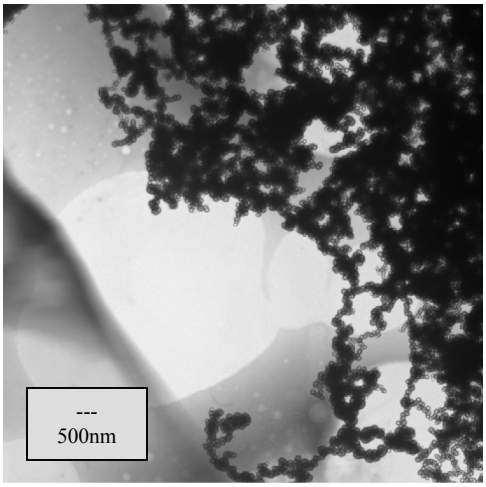

LA w/ NA-MgO

Figure 1.13 TEM images of LA with CM and NA-MgO (1% loadings)

Further evidence of the affect of surface area and/or shape is provided by the image of lactic acid with NA-MgO Plus (Figure 1.14). Long, interconnected strands were not observed in this sample, instead a nearly flower-like structure was observed. It is difficult to analyze exactly how lactic acid reacts with the surface of these materials, but it is obvious that surface reactions are occurring and they have an affect on both the chemical and physical characteristics of the resulting polymer.

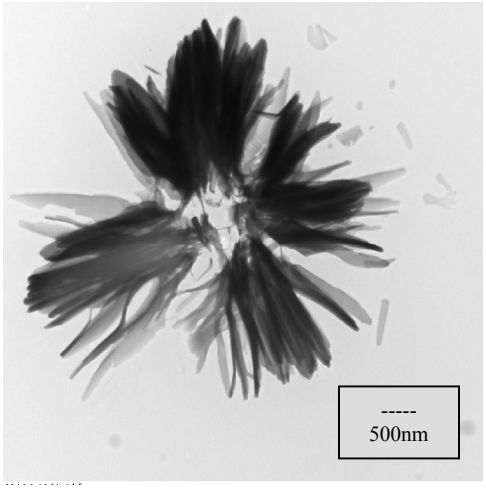

Figure 1.14 LA w/ NA-MgO Plus

In addition to providing the evidence necessary to show the differences created by the addition of highly reactive, large surface area magnesium oxide materials, the IR and TEM analysis also showed that lower loadings of magnesium oxide produced optimum results, therefore 1% loadings were used in all future studies. Additionally, temperature was shown to have an affect on polymerization in section 3.1.1, thus in hopes of further enhancing the polymerization of the composites, methanol was replaced with propanol, as it is a higher boiling point solvent and has similar chemical properties.

3.5 Characterization of LA-MgO composites prepared in propanol

3.5.1 Infrared analysis of composites

Infrared analysis was performed on each of the following: LA w/ CM-MgO, LA w/ NA-MgO, and LA w/ NA-MgO Plus, each with 1% by weight loadings of magnesium oxide (Figures 1.16, 1.17, and 1.18). In addition, infrared analysis was also performed on a lactic acid prepolymer, which contained no magnesium oxide, but otherwise was synthesized under the same reaction conditions (Figure 1.15).

Several similar peaks were observed in each of the samples, including: strong, broad peaks around 3300 cm^{-1}, which are attributed mainly to the hydroxyl functional groups of the lactic acid polymer, as well as excess propanol remaining after the drying step under vacuum; sharp peaks around 1730 cm^{-1} were also observed, indicating the presence of acid or ester functionalities from the lactic acid monomer or newly formed ester linkages of a growing polymer, respectively; peaks were also observed between 1200-1100 cm^{-1}, confirming the presence of ester functionalities. An interesting addition to the spectra for the sample containing

commercial MgO, was that of a strong carboxylate ion signal at 1591 cm^{-1}. Table 1.2 summarizes the peaks observed for each sample.[14]

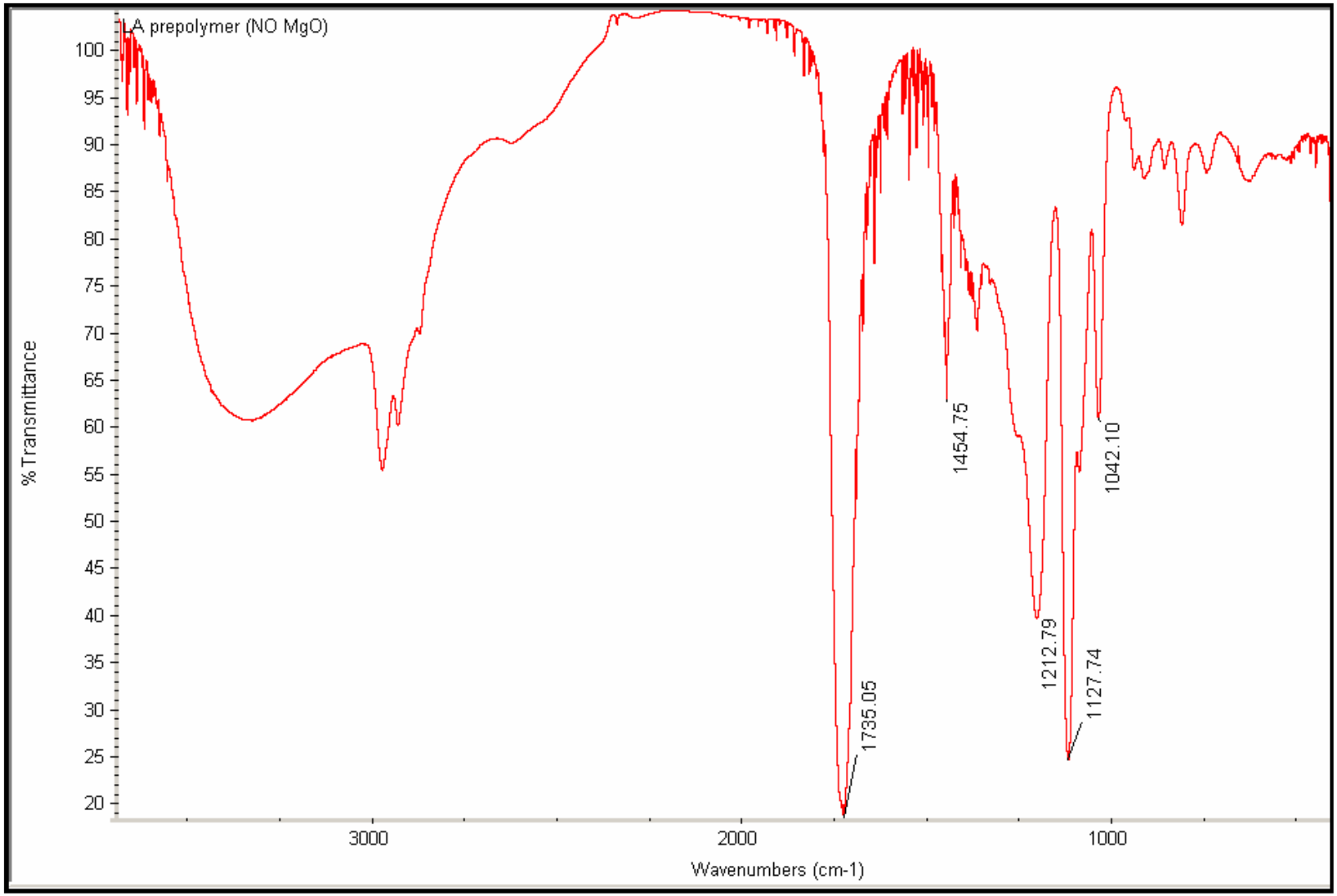

Figure 1.15 Infrared spectra of lactic acid pre-polymer (prepared in propanol)

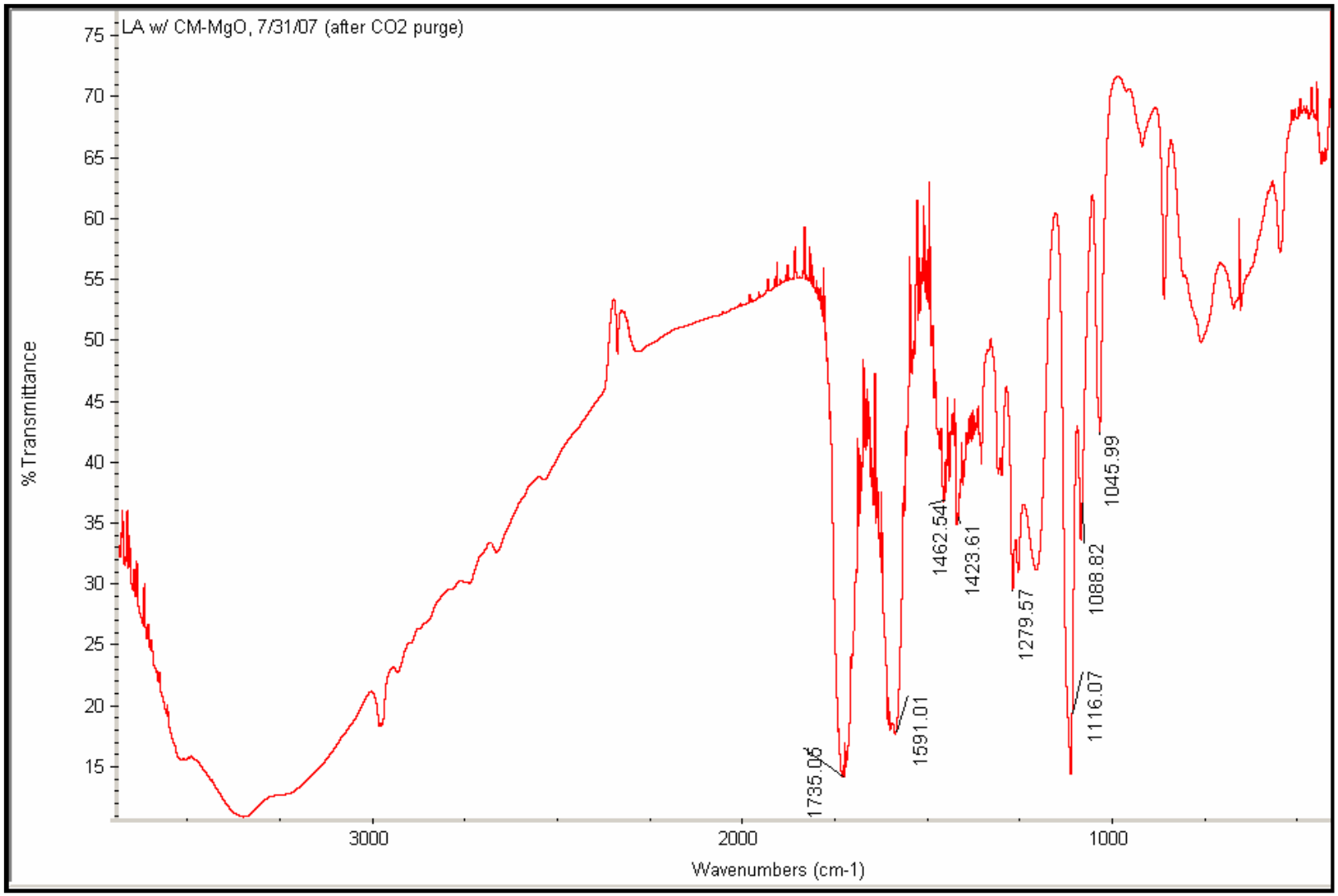

Figure 1.16 Infrared spectra of LA w/ CM-MgO (1% MgO loading, prepared in propanol)

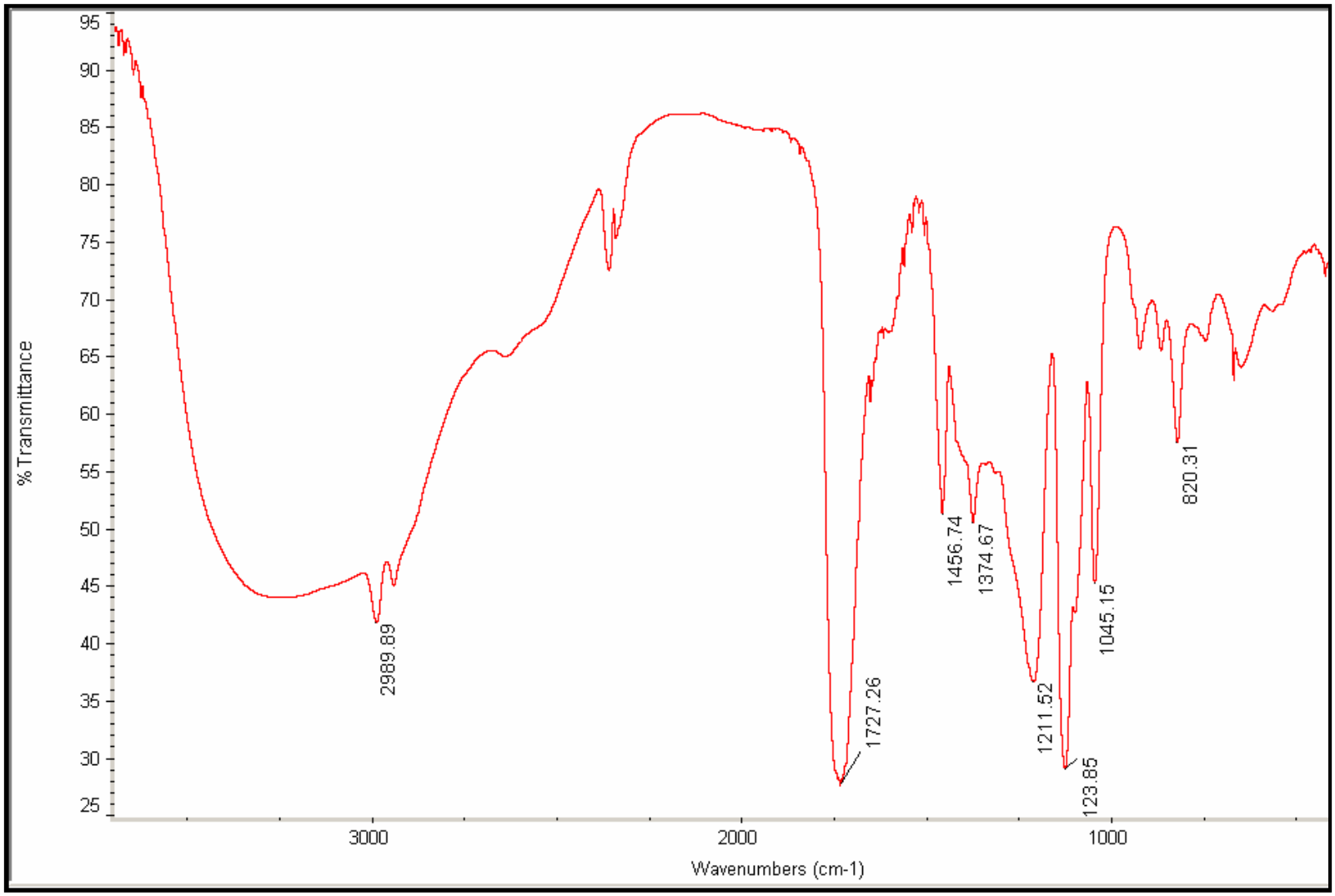

Figure 1.17 Infrared spectra of LA w/ NA-MgO (1% MgO loading, prepared in propanol)

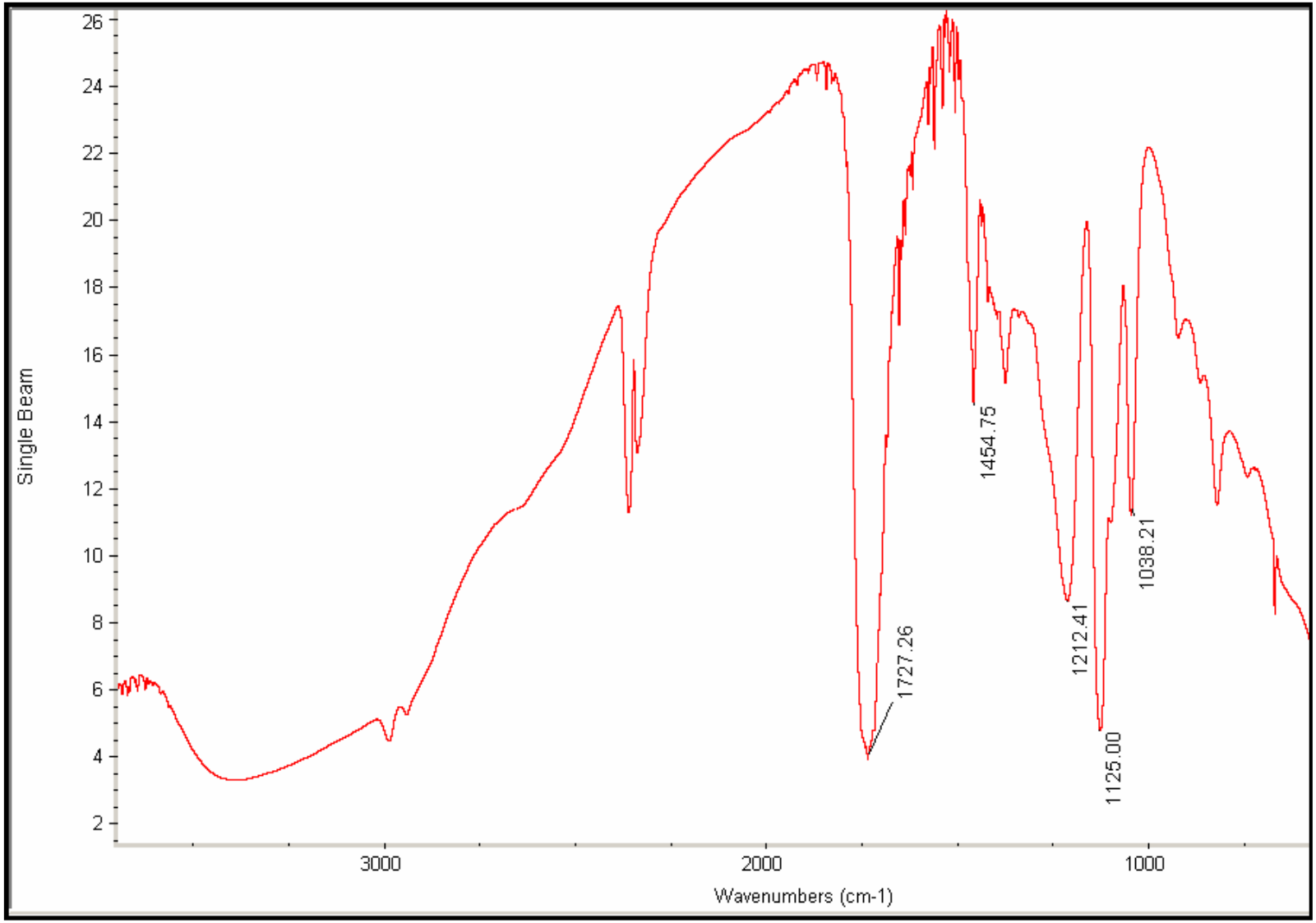

Figure 1.18 Infrared spectra of LA w/ NA-MgO Plus (1% MgO loading, prepared in propanol)

These results indicate that polymerization is catalyzed by the higher temperature reaction conditions achieved by using propanol in place of methanol, as the samples containing Nanoactive® MgO showed strong ester signals and no evidence that carboxylate ion was formed as a product of their reaction with lactic acid, whereas in methanol, infrared analysis indicated that while weak, evidence for the presence of carboxylate ion was present. Interestingly, higher reaction temperatures did not appear to have an affect on the reaction between lactic acid and commercial MgO, as a strong carboxylate peak *was* observed in both the methanol and propanol reaction conditions, which is further confirmation that the size and/or the shape of the Nanoactive® materials influences the pathway that is taken in the reaction between lactic acid and MgO.

3.5.2 NMR analysis of composites

^{1}H and ^{13}C NMR were performed on each of the composites. Additionally, the lactic acid pre-polymer, which contained no magnesium oxide, was also analyzed via NMR. The ^{1}H NMR spectra were particularly useful in identifying differences between the three composites, in addition to providing evidence that the addition of magnesium oxide, in whatever form, *does* have an affect on the polymerization of lactic acid (Figure 1.19 and 1.20).

Figure 1.19 shows the combined spectra of all four samples, while figure 1.20 show expanded sections of the original. The spectra appear in order from bottom to top as follows: lactic acid pre-polymer, lactic acid w/ CM-MgO, lactic acid w/ NA-MgO, and finally, LA w/ NA-MgO Plus. Initially, only minor differences were observed between the four spectra: the triplet located at 3.3 ppm in the pre-polymer spectra completely disappears in the composite samples and the intensities of the peaks vary in each of the four spectra. Closer inspection revealed that these “minor” differences, actually confirm that the surface area and/or shape of the

MgO additive had a definite affect on the polymerization pathway of lactic acid. Further examination of the spectra was necessary in order to determine exactly *how* polymerization was affected by the addition of magnesium oxide nanoparticles, thus a thorough analysis of each of the spectra follows.

3.5.2.1 NMR analysis of lactic acid pre-polymer

In Figure 1.19, a very intense multiplet is present at ~0.86 ppm, but upon expansion (Figure 1.20), a clear doublet (0.87 ppm and 0.82 ppm) of 1:2:1 triplets emerges. These triplets are likely due to $-CH_3$ groups connected to $-CH_2$ methyl functionalities, as is common in propyl groups. The fact that there are two separate methyl peaks indicates there are two similar, but still unique methyl environments. As these are triplets, it is unlikely that these methyl groups are a part of the polymer, thus they confirm the presence of free propanol and perhaps a propyl ester.

The presence of propanol was expected as it was difficult to completely remove all of the solvent from the product. Further evidence for the presence of free propanol was provided by the multiplet at 1.58 ppm ($-OCH_2\mathbf{CH_2}CH_3$) and the triplet at 3.3 ppm ($-O\mathbf{CH_2}CH_2CH_3$). The propyl ester on the other hand, was a question mark for awhile, but upon further study, the formation of a propyl ester is a likely side reaction, as alcohols and acids commonly react to form ester functionalities. It is our belief that after polymerization of lactic acid is exhausted, propyl ester groups are formed from the reaction of the remaining acid functionalities and free propanol, thus termination of the polymerization reaction is achieved by the formation of propyl ester end groups. Further evidence for these groups shows up at 1.6 ppm ($-COOCH_2\mathbf{CH_2}CH_3$) and the triplet at 4.0 ppm ($-COO\mathbf{CH_2}CH_2CH_3$).

Evidence for the presence of the polymer is provided by the overlapping peaks between 1.2 and 1.3 ppm. Several overlapping 1:1 doublets are present in this section of the spectra,

indicating the presence of several similar methyl environments. The doublets indicate that these methyl groups are in close proximity to a -CH group, which is expected as the methyl groups in lactic acid are directly connected to a -CH functionality. The varied chemical shifts of the methyl groups indicate that there were several different polymer environments present in the final product, indicating that perhaps polymerization was stunted by the propanol environment. If this was the case, oligomers could form in many varied sizes, which would change the chemical shifts of the methyl groups slightly. From the expanded spectra (Figure 1.20), it appears that there are four overlapping doublets, indicating the presence of four different polymeric methyl groups. A 1:2:2:1 quartet is also present at ~ 4.0 ppm (overlapping with triplet of propy ester), which confirms the presence of the methyne proton in the lactic acid polymer. In addition to these peaks, there are also several lower intensity peaks in the spectra at ~4.1 and 5.0 ppm which are due to the presence of unreacted lactic acid.

3.5.2.2 NMR analysis of LA with CM-MgO

Upon initial examination of the spectra, it is immediately obvious that very little propanol or propyl ester was present in this sample. The intense peaks between 0.8 and 0.9 ppm are barely visible and the same goes for the multiplet at 1.58 ppm. Additionally, the multiplet centered at 4.0 ppm in the pre-polymer is a clear quartet in this sample, indicating that the methyne proton of lactic acid is still present, but very little if any propyl ester is present. The infrared spectra indicated that carboxylate ion was a primary product of the reaction between lactic acid and commercial MgO, thus it appears that the remaining acid groups were neutralized by the MgO before they could react with propanol to form propyl esters.

As in the pre-polymer spectra, several doublet peaks were observed between 1.2 and 1.3 ppm, indicating the presence of varying polymeric methyl environments, thus it appears that

some degree of polymerization occurred and as before, it appears that several different sizes were produced in the reaction.

3.5.2.3 NMR analysis of LA with NA-MgO and NA-MgO Plus

The spectra for lactic acid with the Nanoactive and Nanoactive Plus samples are slightly different from that of the sample with commercial MgO. The primary difference is that the aforementioned propyl signals (free propanol and propyl ester), while not as intense as those of the pre-polymer, are visible in both spectra, confirming that a decreased number of terminating propyl ester functionalities were formed in the products. The decreased number of terminating groups seems to indicate that polymerization was catalyzed by the addition of the Nanoactive and Nanoactive Plus MgO particles and as a result, longer chain oligomers were formed.

As in the previous samples, several different polymeric methyl environments were identified, but in these cases, the observed doublets exhibited more complicated structure, which shows that the resulting products were very different than the products discussed previously, as clear doublets were observed in both of the previous cases. Perhaps this is a sign that polymerization has occurred on the surface of the particles. After all, if polymerization *did* occur on the surface of the MgO, the methyl environments would be changed as they would be in close proximity to other polymer chains on the surface of the nanomaterials. It is difficult to say exactly how each of these samples differs, but it is obvious that the addition of magnesium oxide, whether in the commercial form or in the nanosized form, has a direct affect on the polymerization of lactic acid.

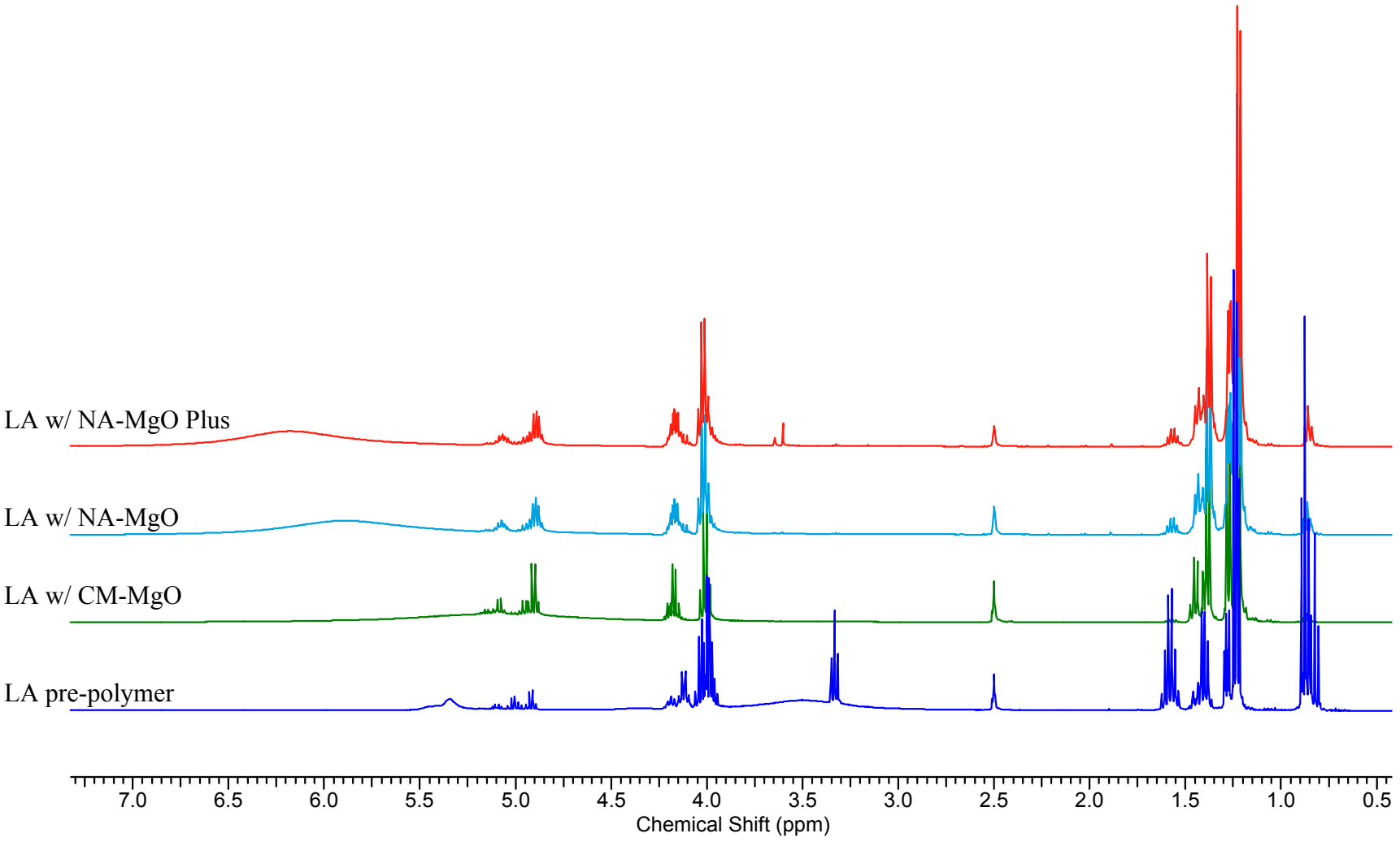

Figure 1.19 NMR spectra of lactic acid – MgO composites

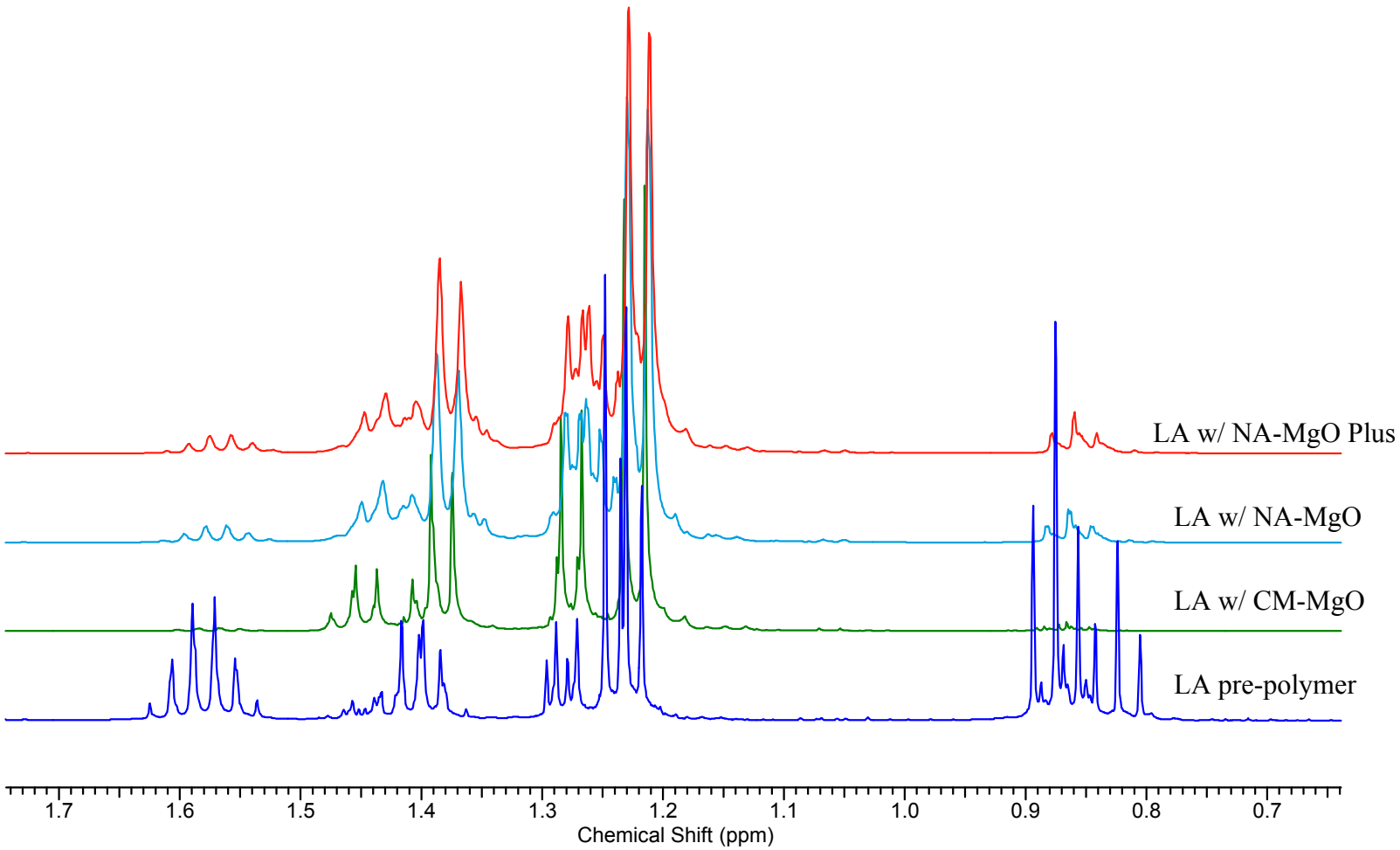

Figure 1.20 Expanded NMR spectra (0.7 – 1.7 ppm) of LA – MgO composites

3.5.3 TEM analysis of composites

Infrared and NMR analysis were very useful in this research as both methods provided a means of confirming which functional groups were present in the products and identifying any obvious differences in the chemical environments of the three composites. However, more information regarding the nature of the reaction as well as the physical changes that occurred by adding MgO to the lactic acid matrix were necessary in order to gain insight into how surface area and shape really affect the polymerization of lactic acid. Therefore, the composites were also examined under a TEM in order to get a better idea of how the chemical differences were manifested on a physical level.

3.5.3.1 TEM analysis: LA with CM-MgO

As with the samples prepared in methanol, very little polymerization was observed, as only short remnants of polymer material are observed. However, the polymeric material appears to be in higher concentration in the samples prepared in propanol than in the previous samples, prepared in methanol (Figure 1.21). Therefore, it can be deduced that while the primary reaction between lactic acid and commercial MgO is an acid-base neutralization reaction, at higher reaction temperatures, polymerization is enhanced, resulting in the observation of more polymeric material on the TEM grid. As before, lactic acid reacts with the available MgO in a neutralization reaction and then the remaining lactic acid is polymerized via the application of heat. In this case, polymerization was initiated at numerous sites due to the higher reaction temperature, which results in the vast number of polymer units observed under the microscope.

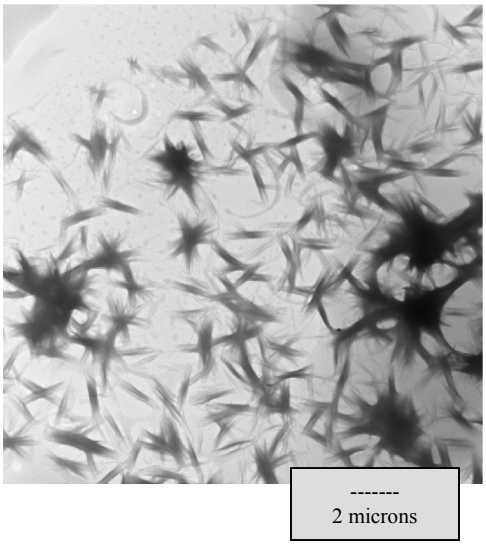

LA w/ CM-MgO (1% loading)
Prepared in propanol

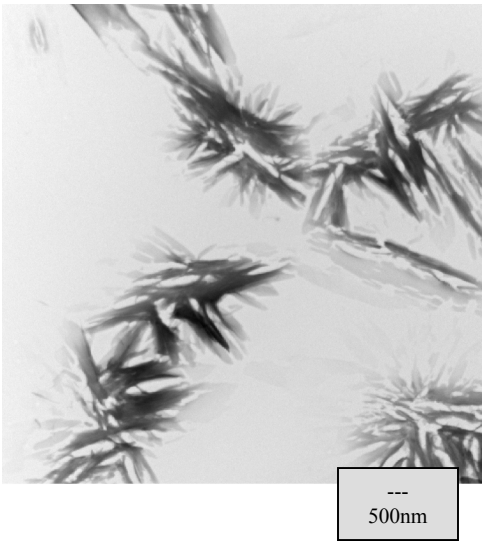

LA w/ CM-MgO (1% loading)
Prepared in methanol

Figure 1.21. TEM images of LA w/ CM-MgO (1% loadings)

3.5.3.2 TEM analysis of LA w/ NA-MgO

In methanol, Nanoactive® MgO performed very well, as long-chain, interconnected polymer strands were observed, indicating that the presence of the nanomaterial catalyzed polymerization of the monomer. At higher temperatures (in propanol), the effect of adding NA-MgO was even greater, as 1.22 shows. Long-chain, highly interconnected and crosslinked materials can be seen in the image, indicating that polymerization was further catalyzed by the higher reaction temperature. Additionally, by comparing Figure 1.21 with Figure 1.22, it is easy to see that the products physically, are very unique and this uniqueness *must* be due to the differences in surface area and/or shape of the magnesium oxide additive. If our hypothesis is correct, initiation of polymerization occurs at the surface of the particles, which would produce

several strands on the surface of a particle, which could then interconnect and crosslink, much like that which is observed in the TEM image.

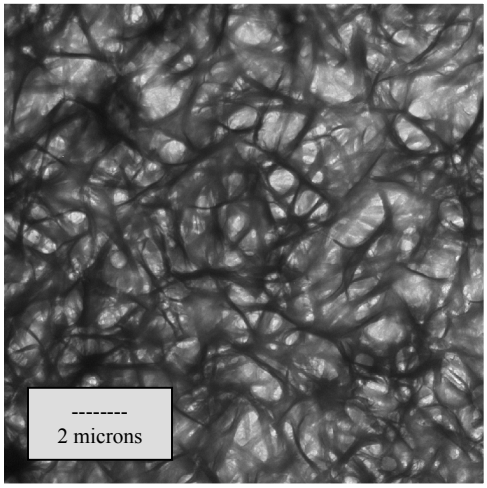

LA w/ NA-MgO (1% loading)
Prepared in propanol

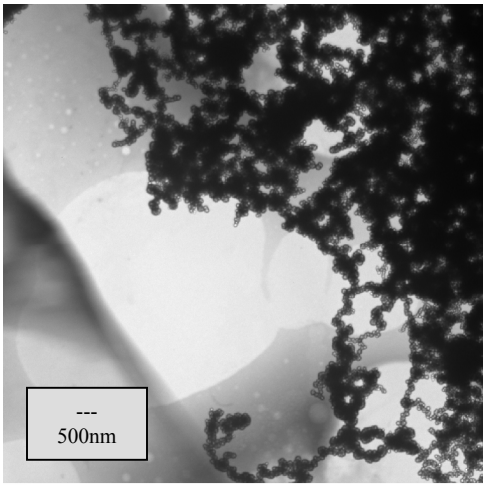

LA w/ NA-MgO (1% loading)
Prepared in methanol

Figure 1.22 TEM images of LA w/ NA-MgO (1% loadings)

3.5.3.3 TEM analysis of LA w/ NA-MgO Plus

Further evidence of the affect of surface area and/or shape is provided by the image of lactic acid with NA-MgO Plus (Figure 1.23). As in the sample prepared in methanol long, interconnected strands were not observed, instead unique structures were formed. In propanol, star-shaped materials were observed, whereas in methanol, flower-like materials were the norm. Both of these materials have voids in the center and as a result, it is difficult to analyze exactly how lactic acid reacts with the surface of these materials, as NA-MgO Plus is a fibrous material, as shown in Figure 1.3. It is possible that during reflux, the nanoparticles interact with each other to form a circular structure, which the lactic acid then reacts with. In this case, polymerization still initiates on the surface of the material and then continues until termination

occurs. Again, it is obvious that surface reactions are occurring and they absolutely have an affect on the physical characteristics of the resulting polymer.

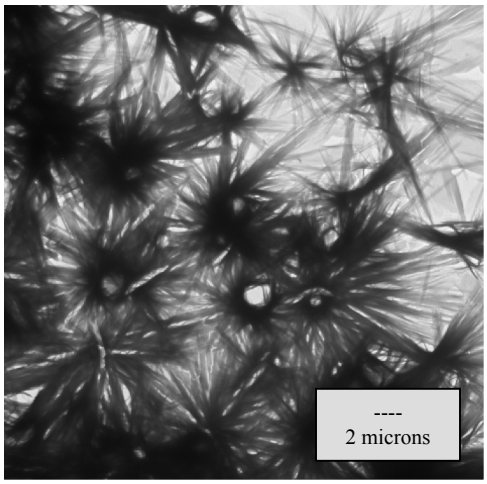

LA w/ NA-MgO Plus (1% loading)
Prepared in propanol

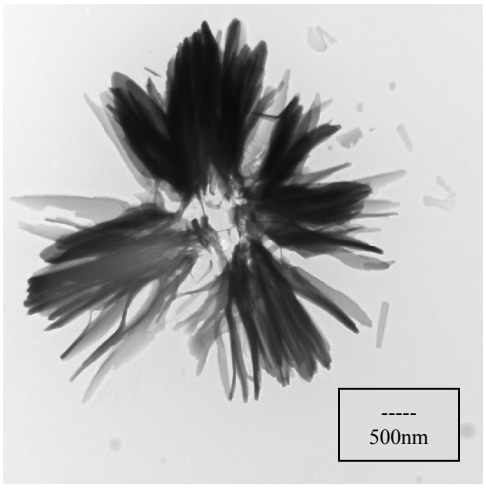

LA w/ NA-MgO Plus (1% loading)
Prepared in methanol

Figure 1.23 TEM images of LA w/ NA-MgO Plus (1% loadings)

3.5.4 UV-Vis analysis of composites

Each of the composites, along with the prepolymer control and the lactic acid monomer starting material were analyzed via UV-Vis spectroscopy. Figure 1.24 shows that addition of magnesium oxide shifts the absorption maximum from ~290 nm to 255 nm. An additional shoulder is also evident in the composite containing CM-MgO, indicating the presence of more than one product. As discussed previously, commercial MgO is likely to react with lactic acid to form a lactate salt, however, polymerization of lactic acid is also expected, the result of which is two products. The peak at ~290 nm is likely due to unreacted lactic acid, as the absorption maximum of the pure monomer is near 290 nm as well. The red-shifted portion of the spectra

which appears upon the addition of magnesium oxide is therefore a result of the formation of a lactic acid – magnesium oxide composite.

The UV-Vis data provides further evidence that the addition of a Nanoactive form of MgO changes the nature of the resulting composite even more so than commercial MgO. With the addition of NA-MgO, a broadened, single peak is observed, the maximum of which is slightly red-shifted. This indicates that the surface area and/or the difference in shape of the nanocrystals has catalyzed the formation of the polymer composite. However, the broadness of the peak points to the presence of several different sizes of polymer. The TEM images of the material seemed to indicate this as well, with numerous highly branched and interconnected polymer strands visible under the microscope.

In contrast, the composite containing NA-MgO Plus produces a symmetrical peak with a maximum absorption at ~280 nm. The symmetric nature of the peak and the location of the absorption peak value indicates not only that NA-MgO Plus catalyzes polymer formation, but also that the products of the reaction are uniform in size. The TEM images of these materials confirm these results, as a myriad of similarly sized, star-shaped materials were observed when examining these composites under the microscope.

The UV-Vis data summarized above offers further confirmation that the addition of nanomaterials to a biomolecule like lactic acid does in fact catalyze polymerization and it appears from these data that the surface area and reactivity of the nanomaterials,affects catalysis the most. It also confirms the TEM results indicating that the materials formed are the most uniform when NA-MgO Plus is added.

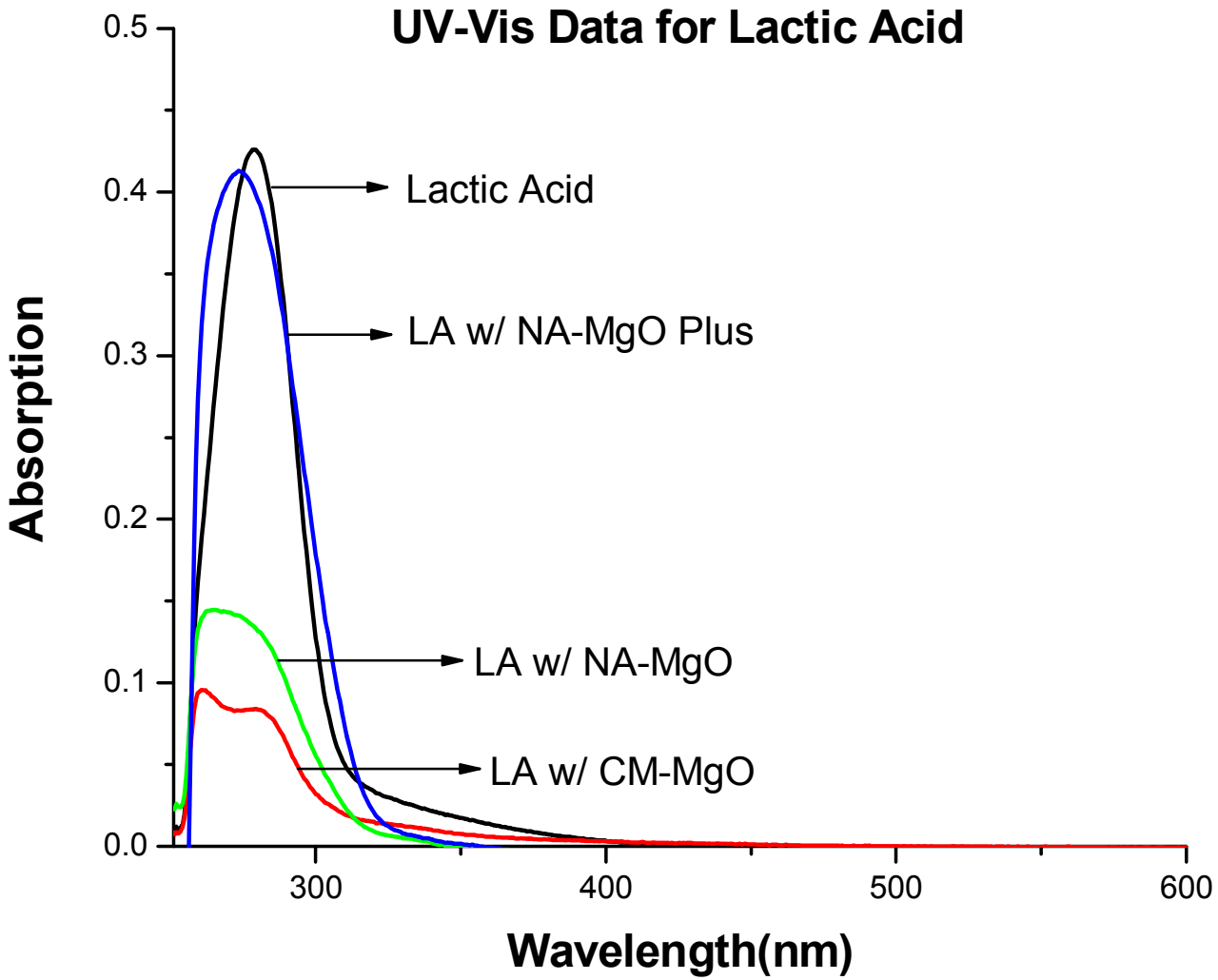

Figure 1.24 Plot of UV-Vis data for lactic acid and LA-MgO composites

3.5.5 Thermal Analysis via TGA and DSC Analysis

3.5.5.1 Melting and Crystallization Properties

All of the lactic acid – magnesium oxide composites showed melting temperatures in the first heat-scanning (Figure 1.25). The prepolymer composite with NA-MgO Plus had the sharpest melting peak while the composite with CM-MgO presented two broad melting peaks. In between the two extremes, the composite containing NA-MgO produced a single, slightly broadened melting peak. The second heating scan produced very different results. Figure 1.25 shows that a melting peak, while slightly lower than in the first heating scan, was observed for the NA-MgO Plus composite, while no melting temperatures could be derived for the remaining composites. These phenomena suggest that lamellae were formed due to rearrangement of the prepolymer macromolecular chains. The weakening or disappearance of the melting peaks for the composites with CM-MgO and NA-MgO could be caused by pyrolysis of the prepolymer chains. The sharpness of the melting peaks also indicates that the lamellae formed in the prepolymers with NA-MgO Plus and NA-MgO were more uniform in molecular weight than that of the composites with CM-MgO.

Perhaps the most interesting data however, is the actual melting temperatures, summarized in Table 1.3. The highest melting point was observed in the prepolymer composite with NA-MgO Plus, which suggests that the the star-shaped lamellae observed in the TEM are more uniform and thermally stable than the other two composites. In addition, the composite containing NA-MgO Plus showed the largest melting enthalpy, while the prepolymer with CM-MgO had the smallest melting enthalpy indicating that the percentage lamellae formed in the prepolymer with NA-MgO Plus was higher than that in the prepolymer with CM-MgO.

Table 1.3 DSC analysis of lactic acid – MgO composites

Sample		T_c (°C)	T_m (°C)	ΔH_m (J/g)
LA w/ CM-MgO	First heating scan	60.6	150.7 162.3	14.08
	Second heating scan	30.1	153.1	8.38
LA w/ NA-MgO	First heating scan	---	158.8	31.04
	Second heating scan	---	---	---
LA w/ NA-MgO Plus	First heating scan	---	162.6	40.24
	Second heating scan	34.4	158.5	31.04

In addition to the melting properties, Table 1.3 also shows cold crystallization temperatures for the three composites. A small cold crystallization peak for the prepolymer with CM-MgO was observed in the first heating scan, which suggests that its crystallization rate was the lowest of the three. A cold crystallization peak was also observed for the prepolymer with NA-MgO Plus in the second heating scan, suggesting that the material crystallized readily upon heating. No cold crystallization peak was observed for the prepolymer with NA-MgO, implying that the composite could not crystallize as a result of serious pyrolysis of the prepolymer chains.

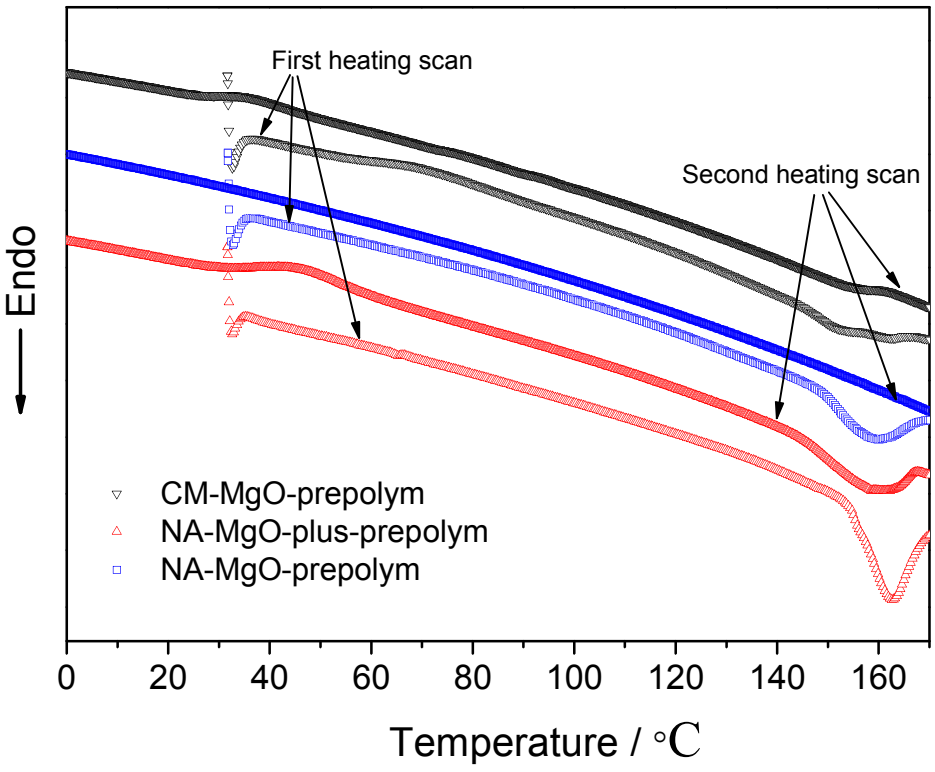

Figure 1.25 DSC curves for Lactic acid – MgO composites

3.5.5.2 Thermal Stability

TGA analysis of the three composites strongly suggests that thermally stable complexes were in fact formed when nanoparticles of magnesium oxide were reacted with lactic acid. Figure 1.26 shows that complexes were formed with both NA-MgO and NA-MgO Plus and the complexes formed exhibited very high decomposition temperatures ranging from 400 to 520°C (Table 1.4). The composite decomposition temperatures were separated from the dehydration of pure MgO particles via comparison. As shown in Figure 1.26, each of the three MgO particles decomposed slightly between the temperatures of 255°C and 400°C, which suggests that the decomposition occurring around 500C is due to the new complex formed between lactic acid and the MgO particles. Interestingly, it appears that a greater amount of composite was formed in

the reaction between NA-MgO and lactic acid, as a higher weight loss was observed within this temperature range, 78.5%, compared with the NA-MgO Plus and CM-MgO, with 70.5% and 22.8% weight losses, respectively.

The decomposition of the MgO composites follows a three step pattern and while some of the observed weight losses at lower temperatures may be attributed to the pyrolosis of the hydroxyl groups on the surface of the nanocrystals, the first step at low temperature (~90°C – 290°C) is most prominently due to the decomposition of unreacted lactic acid, which both the NMR and IR results indicate is present. Unfortunately, thermal analysis via TGA cannot be performed on pure lactic acid, as it is in liquid form, so it was not possible to compare patterns. However, unreacted lactic acid is the most probable to decompose in this temperature range as the boiling point of the liquid is ~122°C.

The second step, between 330°C and ~400°C, may be attributed to the decomposition of one form of the lactic acid-MgO composite produced in the reaction. As shown in the TEM images of these materials, each composite took on a different shape and probably very different molecular weights, thus several different sizes of polymer were likely formed. Therefore, this step is likely due to the decomposition of the lower molecular weight portions of the composite.

The third and final step of the decomposition of these composites occurs at very high temperatures and might be ascribed to the decomposition of the polymers with a higher degree of crosslinking, which would explain why a higher a weight loss was observed with the composite containing NA-MgO. Additionally, the decomposition rate of the prepolymer with NA-MgO is much faster than that with NA-MgO Plus, which confirms the stability results observed in the DSC.

Table 1.4 TGA analysis of lactic acid – MgO composites

Sample	Step 1			Step 2			Step 3		
	T_{onset} (°C)	T_{end} (°C)	W_{loss} (%)	T_{onset} (°C)	T_{end} (°C)	W_{loss} (%)	T_{onset} (°C)	T_{end} (°C)	W_{loss} (%)
CM-MgO	255	355	4.2	NO DATA					
NA-MgO	262.1	367.3	13.3						
NA-MgO Plus	285.7	390.9	22.9						
LA Prepolymer	52.4	354.0	92.7						
CM-MgO Prepolymer	92.9	275.4	34.0	362.8	387.3	33.9	403.0	493.6	22.8
NA-MgO Prepolymer	91.7	290.5	62.4	348.0	397.5	63.4	439.2	520.8	78.5
NA-MgO Plus Prepolymer	91.1	287.5	42.0	334.7	392.1	50.2	439.2	520.8	70.5

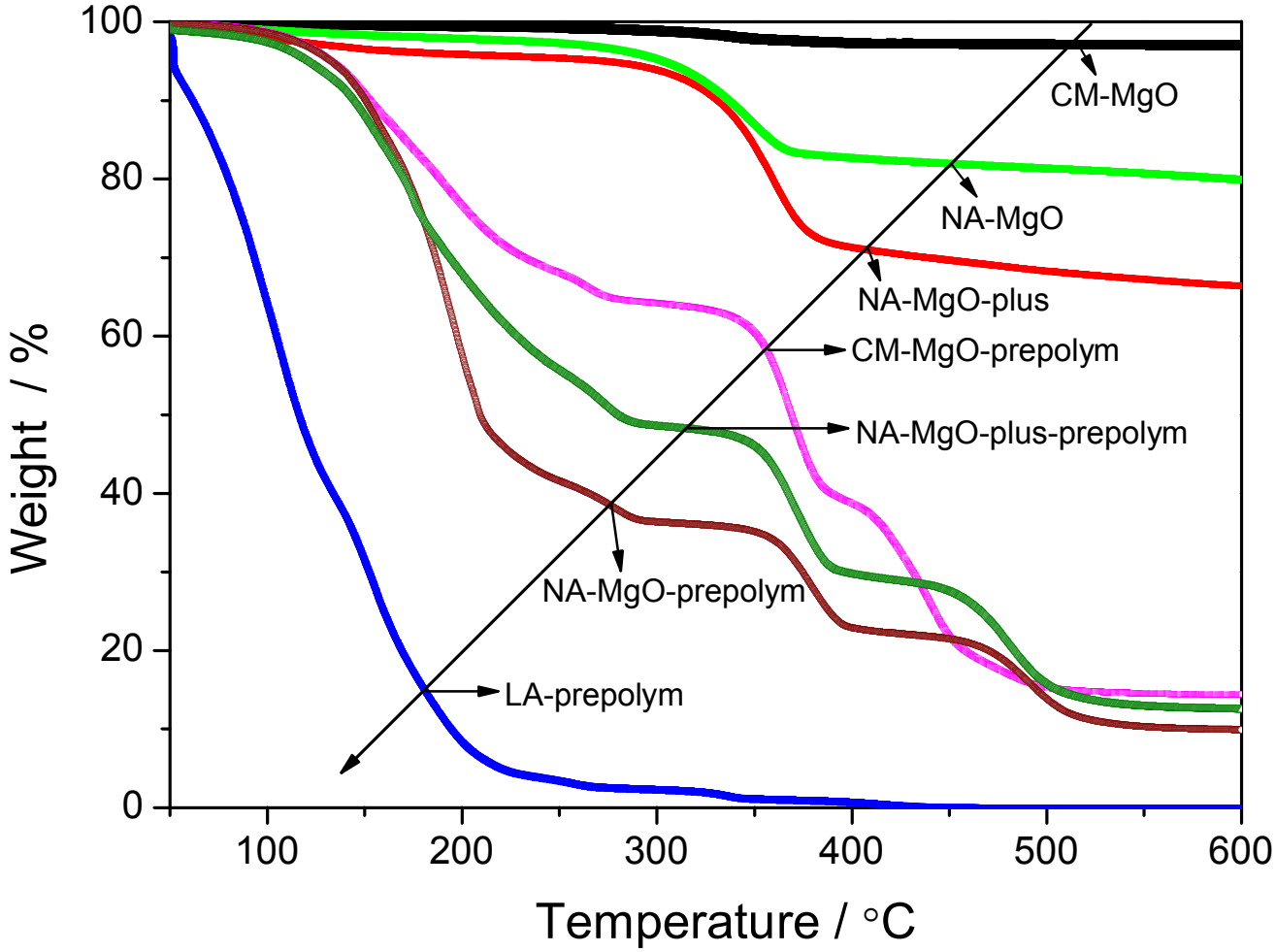

Figure 1.26. TGA of lactic acid – MgO composites and pure MgO samplesa

CHAPTER 4 - Conclusions and Future Work

The areas of biopolymers and nanotechnology are interesting and unique in and of themselves, but the combination of the two is revolutionary. Several papers have been published regarding the use of nanoclays in petroleum-based polymers and plastics[4,7-11] but the use of metal oxide nanoparticles in biopolymers is very new and exciting.

Our research focused on the use of magnesium oxide as an additive to the biopolymer, lactic acid. Of particular interest was the chemistry that occurred between the two. NMR, FTIR, UV-Vis, and TEM were all used to characterize the chemical differences resulting from the addition of Commercial, Nanoactive®, or Nanoactive Plus® magnesium oxide.

Titrations of lactic acid were performed with each of the three types of MgO in addition to the testing listed above. The results of the titrations indicated that the surface area and reactivity of the different materials had an affect on the reaction pathway. For example, commercial MgO neutralized the most lactic acid with the least amount of material indicating that the primary reaction between lactic acid and commercial MgO is a neutralization reaction. In contrast, more material was required to reach an equivalence point with the nanoactive samples, confirming that while a neutralization reaction still occurs, there are also competing surface reactions between the lactic acid and the surface –OH groups. These surface reactions appear to be the points of initiation for polymerization of lactic acid on the surface of the MgO nanoparticles.

With this in mind, NMR and IR analysis were performed on each of the different composites in order to confirm these results. At high temperatures, a strong carboxylate peak in the sample containing commercial MgO was obvious, but very little evidence of carboxylates

was observed in the composites with the nanoactive MgO samples, confirming that an acid-base reaction was not the primary pathway in the reaction between lactic acid and the MgO nanoparticles. Additionally, NMR analysis showed very complex methyl environments in the nanocomposites, indicating that substantially different materials were produced with each material.

TEM provided perhaps the most interesting piece of the puzzle. The images indicate that not only does the surface area of the additive affect the chemical properties of the resulting composites, but also the physical properties. The images show that the composites with nanoparticles produced materials with high polymer content, as expected from the previous results. However, the initiation of polymerization appears to be different with each material, as long, interconnected strands were observed in the composites containing NA-MgO, and circular, star-shaped materials were observed with NA-MgO Plus. This indicates that in addition to surface area, the *shape* of the nanoparticles also affects the resulting physical and chemical properties of the composites.

Thermal stability was also an important part of this study, as one of the issues with the use of lactic acid is its stability when heated above its glass transition temperature. TGA and DSC analysis were performed in order to examine how the addition of nanoparticles affects this stability. The results indicate that thermally stable materials, with decomposition temperatures above 400°C were produced in this study. Unfortunately, time constraints did not allow us to compare the results achieved with the nanocomposites with that of PLA, which is of course the end goal.

The future of this project lies primarily in furthering the polymerization of the prepolymer nanocomposites made in this study to form PLA. The chemical, physical, thermal,

and rheological properties of the full polymers could then be compared with that of commercial PLA. Additionally, other inert metal oxide nanoparticles, such as titania, have potential as additives to biopolymers. This work is still in its infancy, but has definite potential to both change and improve the nature and use of bioplastics.

CHAPTER 5 - References

1. Wool, Richard P.; Sun, Xiuzhi Susan; Bio-Based Polymers and Composites, Elsevier Publishing, New York, 2005.

2. Johnson, R.M.; Mwaikambo, L.Y.; Tucker, N.; Biopolymers, 2001, 1-25.

3. Klabunde, K.J.; Nanoscale Materials in Chemistry, Wiley-Interscience Publications, New York, 2001.

4. Vasudeo, Y.B.; Rangaprasad, R.; Popular Plastics and Packaging, Nov. 2005, 127-146.

5. Ray, S.S.; Bousmina, M.; Progress in Materials Science, 2005, 50, 962-1079.

6. Avella, M.; Errico, M.E.; Gentile, G.; Macromolecular Symposium, 2007, 247, 140-146.

7. Ton-That, M.T.; Perrin-Sarazin, F.; Cole, K.C.; Bureau, M.N.; Denault, J.; Polymer Engineering and Science, 2004, 44, 1212-1219.

8. Kawasumi, M.; Hasegawa, M.; Kato, A.; Usuki, A.; Okada, A.; Macromolecules, 1997, 30, 6333.

9. Kato, M.; Okamoto, H.; Hasegawa, N.; Usuki, A.; Polymer Engineering and Science, 2003, 43, 1312.

10. Yano, K.; Usuki, A.; Okada, A.; Kurauchi, T.; Journal of Polymer Science, Part A: Polymer Chemistry Ed., 1993, 31, 2493.

11. Biasci, L.; Aglietto, M.; Ruggeri, G.; Ciardelli, F.; Polymer, 1994, 35, 3296.

12. http://edis.ifas.ufl.edu. Accessed 10/25/07

13. Jeevanandam, P.; Mulukutla, R.S.; Yang, Z.; Kwen, H.; Klabunde, K.J.; Chemistry of Materials, 2007, 19, 5395, 5403.

14. Silverstein, R.M.; Webster, F.X.; Kiemie, D.J.; Spectrometric Identification of Organic Compounds. John Wiley and Sons, 2005.